Покмарки (выбоины, оспины) (Pockmarks)

А.М. Никишин

Pockmarks are craters in the seabed caused by fluids (gas and liquids) erupting and streaming through the sediments.

Pockmarks were discovered off the coasts of Nova Scotia, Canada in the late 1960s by Lew King and Brian McLean of the Bedford Institute of Oceanography.

Pockmarks are uncommon on the land surface, and are expected in the ocean.
They were discovered off Nova Scotia, using a new side scan sonar developed in the late 1960s by Kelvin Hughes.
The craters off Nova Scotia are up to 150 m (490 ft) in diameter and 10 m (33 ft) deep.
Pockmarks have been found worldwide.
Discovery was aided by the use of high-resolution multibeam acoustic systems for bathymetric mapping. In these cases, pockmarks have been interpreted as the morphological expression of gas or oil leakage from active hydrocarbon system or a deep overpressured petroleum reservoir

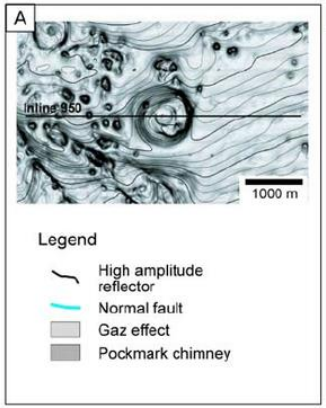
A
Inline 950
1000 m
Legend
High amplitude reflector
Normal fault
Gaz effect
Pockmark chimney

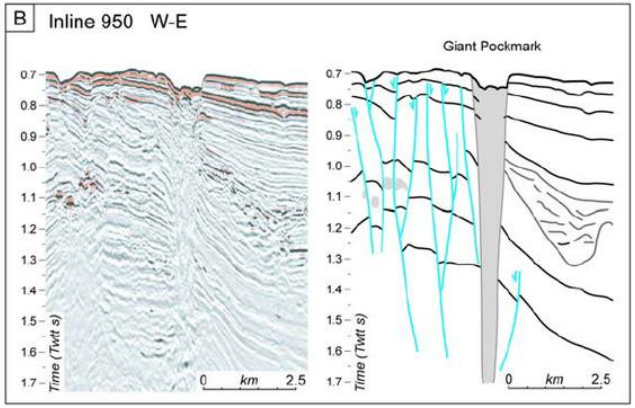
B
Inline 950 W-E
Giant Pockmark
Time (Twtt s)
0 km 2.5

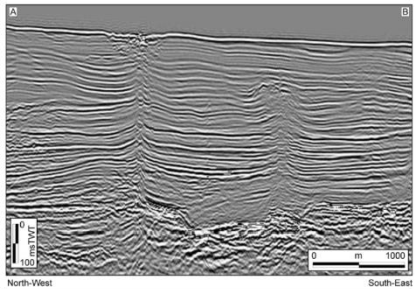
A
B
ms TWT
0 m 1000
North-West
South-East

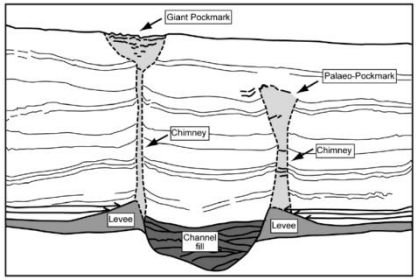
Giant Pockmark
Palaeo-Pockmark
Chimney
Chimney
Levee
Channel fill
Levee

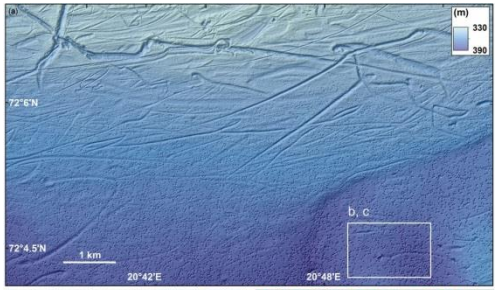
(a)
(m)
330
390
72°6'N
72°4.5'N
1 km
20°42'E
20°48'E
b, c

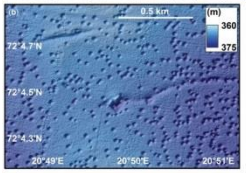
(b)
0.5 km
(m)
360
375
72°4.7'N
72°4.5'N
72°4.3'N
20°49'E
20°50'E
20°51'E

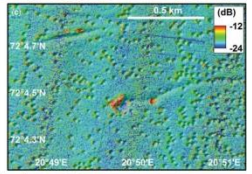
(c)
0.5 km
(dB)
-12
-24
72°4.7'N
72°4.5'N
72°4.3'N
20°49'E
20°50'E
20°51'E

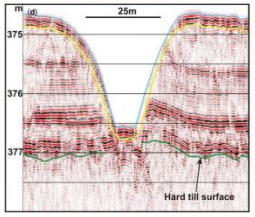
m
(d)
25m
375
376
377
Hard till surface


(e)
Barents Sea
Norwegian Sea
Norway
70°N
60°N
North Sea
10°E
20°E

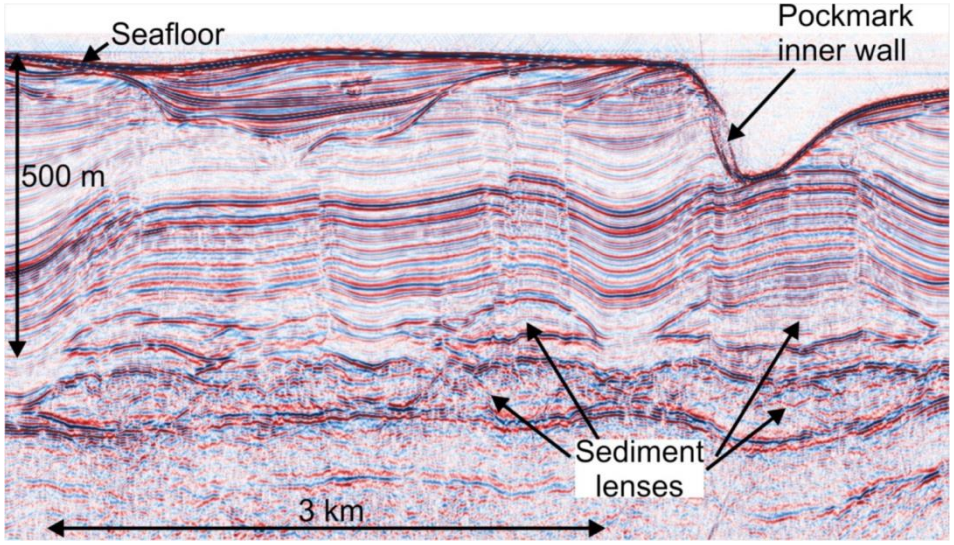
Seafloor
Pockmark inner wall
500 m
Sediment lenses
3 km

Pockmarks

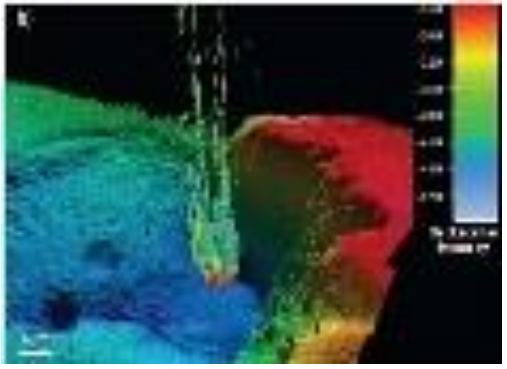

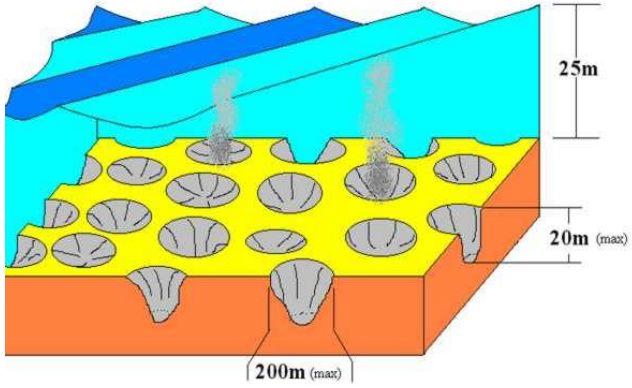
25m
20m (max)
200m (max)

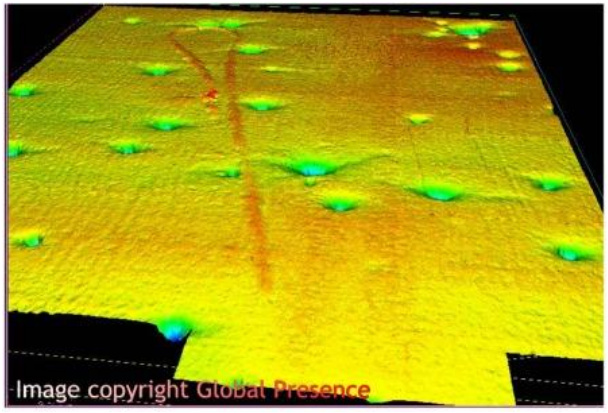
Image copyright Global Presence

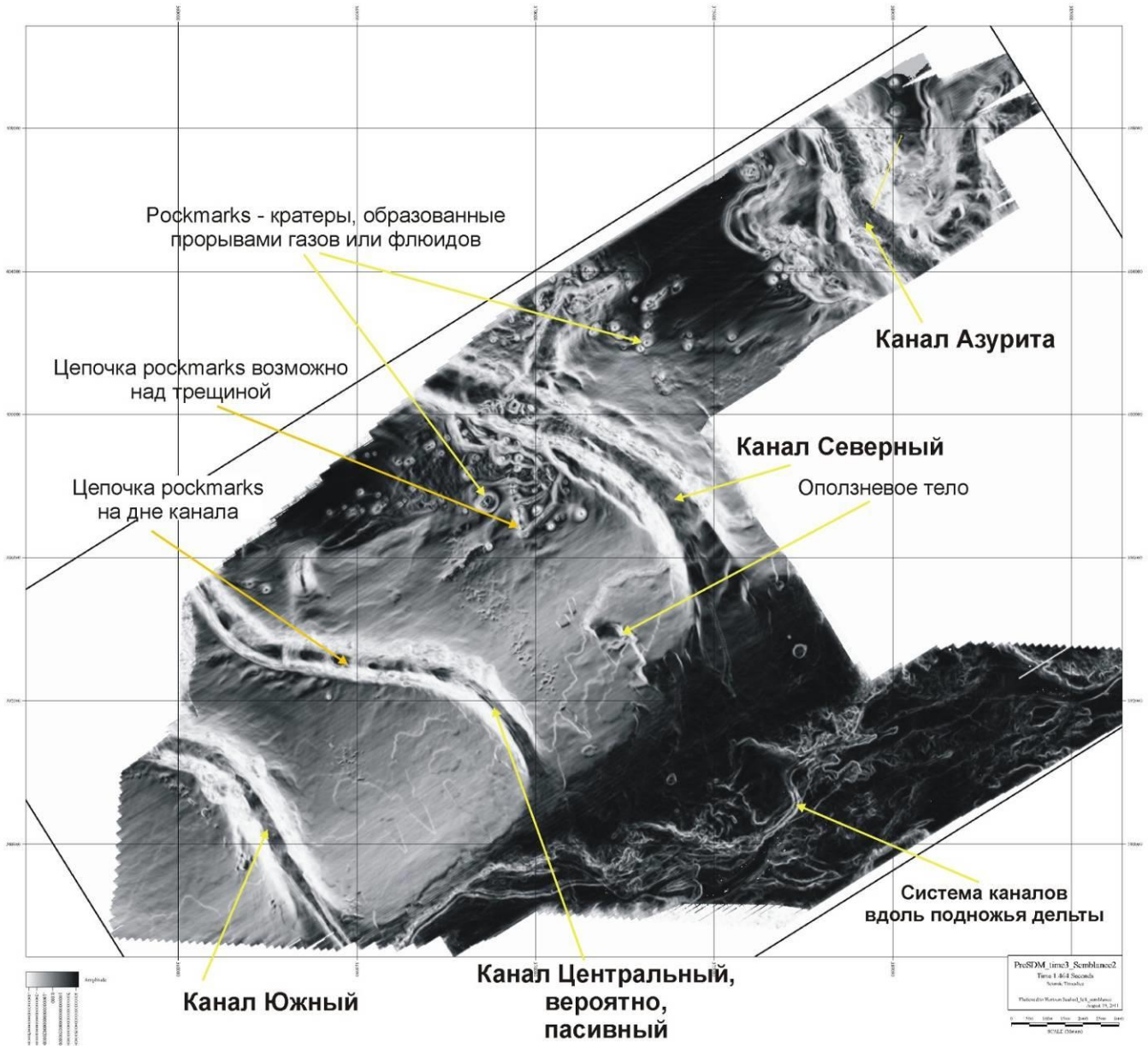

Рельеф часть дельты Нигера, показанный в виде карты когерентности. Видны в целом прямолинейные каналы. Широко распространены покмарки. Иногда они образуют цепочки на дне каналов.

А.М. Никишин, В. Никитина

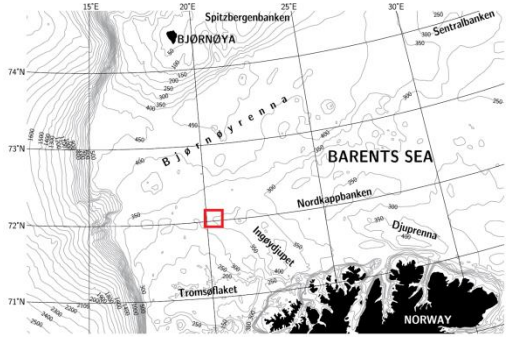

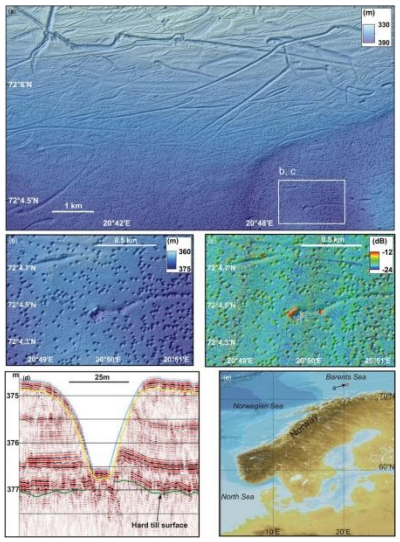

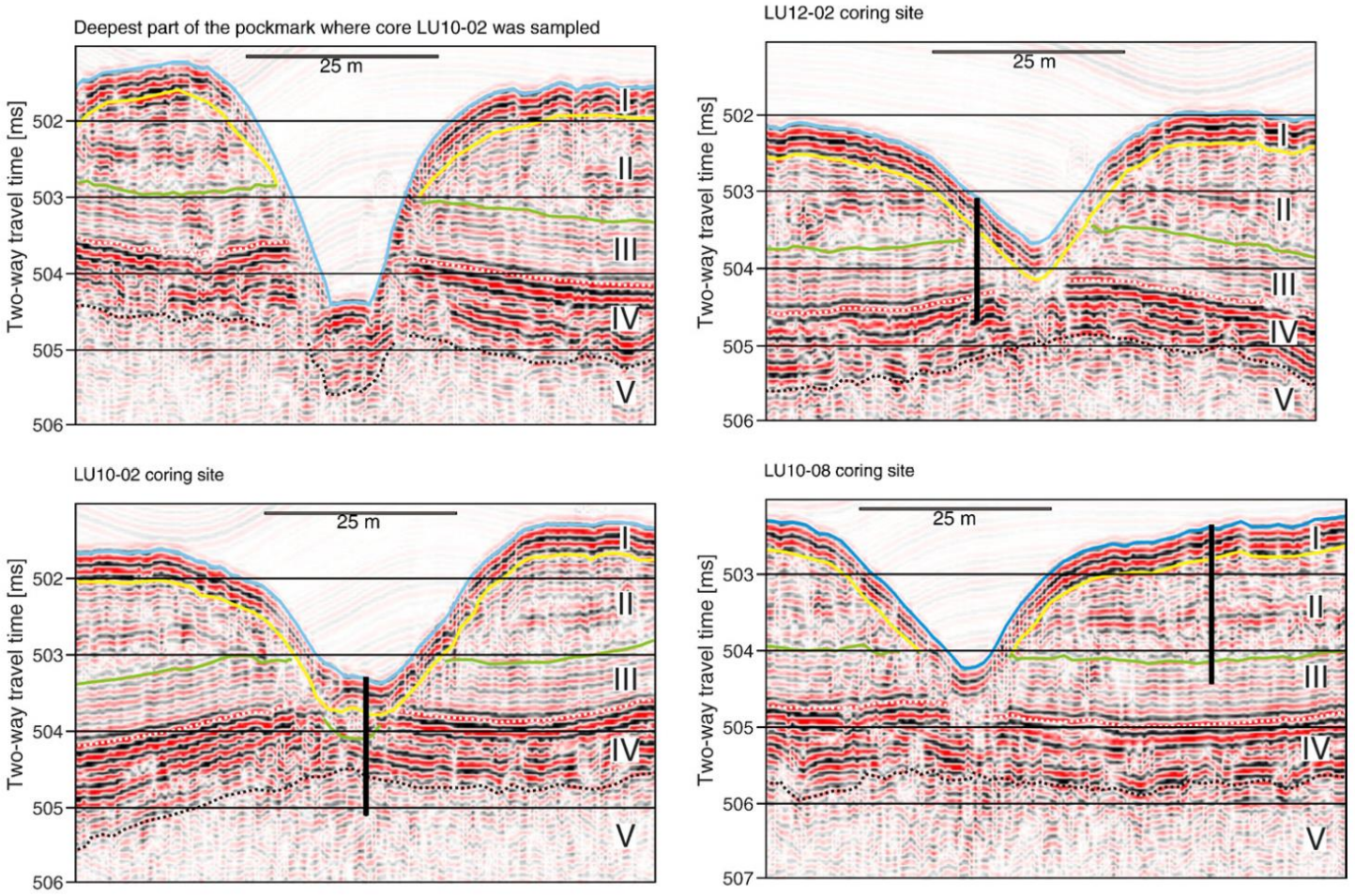

Fig. 12. W–E oriented high resolution seismic images with seismic units marked. The vertical axis shows the calculated two-way traveltime (TWT) from the sea surface, using a velocity of 1470 ms^{-1} for the water column. The depth of the cores (black bars) was converted to TWT using a velocity of 1500 ms^{-1}, and assuming a 220 cm length for core LU09-402 and 160 cm length for core LU09-450.

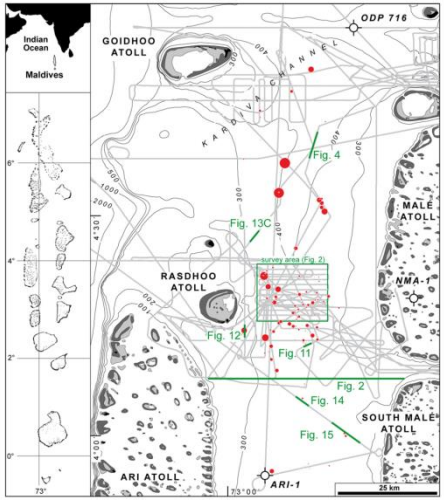

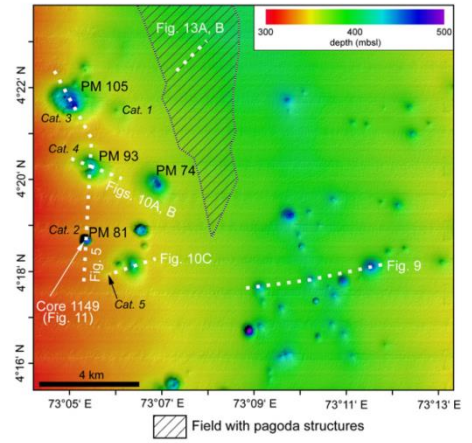

Fig. 3. Multibeam map of the pockmark area located West of Rashdoo Atoll, with numbers of pockmarks discussed in the text. Figure numbers refer to location of sections and multibeam images.

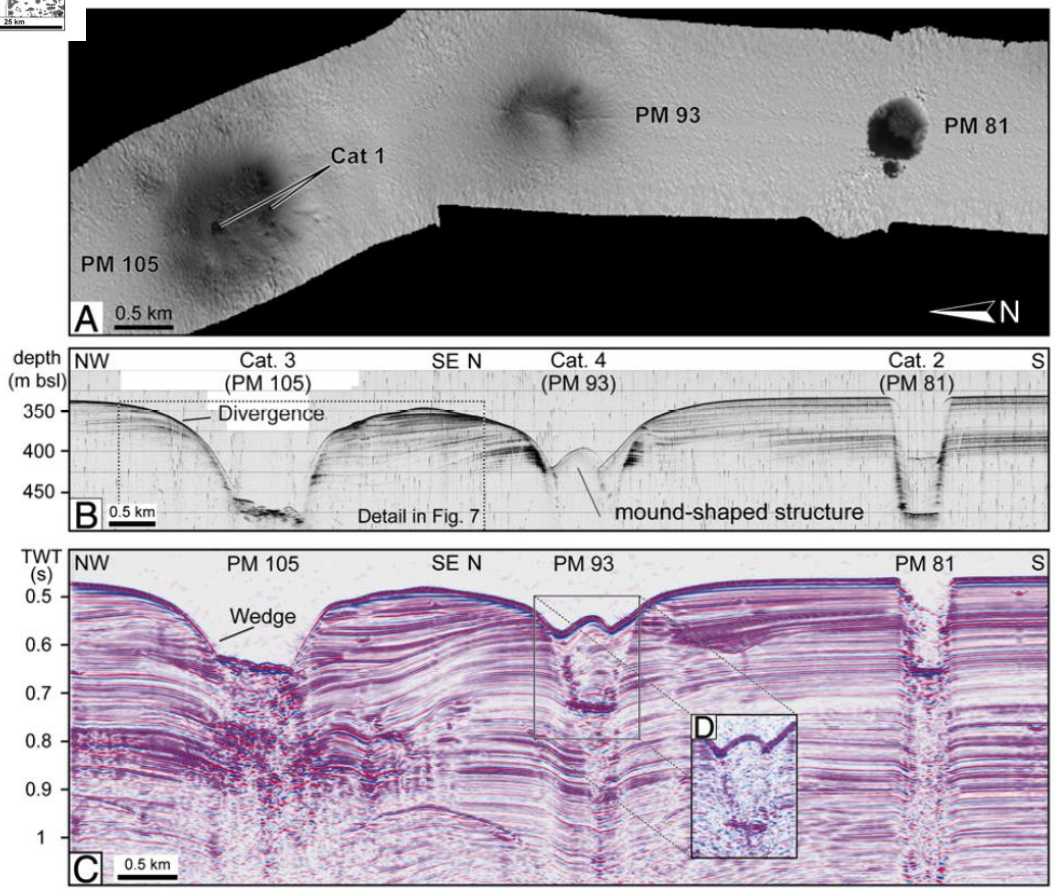

Fig. 5. A: Multibeam image of category 2, 3 and 4 structures. B: Parasound section through the same structures as shown in A. Note the medium amplitude reflection within the Category 2 structure (PM 81). C: MCS section through the same pockmarks as shown in A and B. See text for discussion.

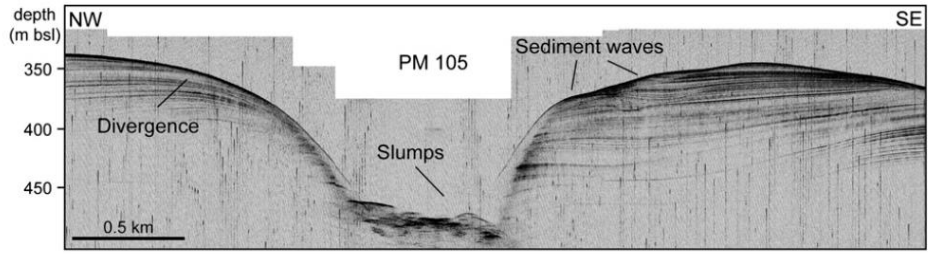

Fig. 7. Cross section (Parasound) of a Category 3 structure. At the bottom of the structure there are mounded and discontinuous reflections, interpreted as slumps. Layering around the structure is characterized by divergent layering and sediment waves. These bedding geometries reflect erosion and reworking of sediment around the crater by bottom currents.

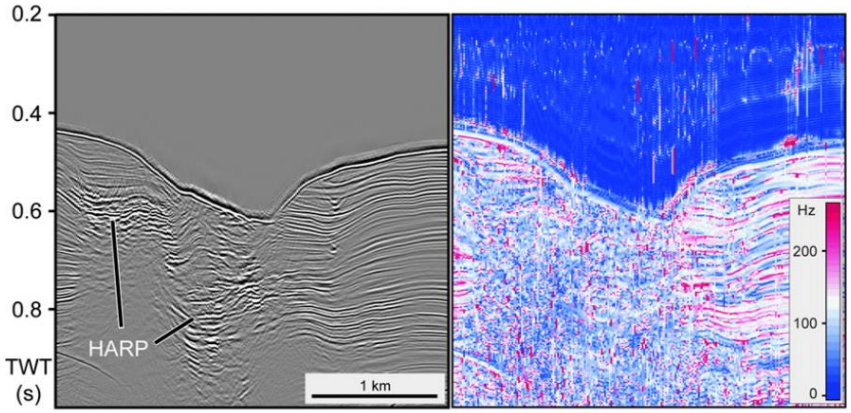

Fig. 8. MCS section through a Category 3 pockmark (A) with the corresponding instantaneous frequency (B). Note reduction of the instantaneous frequency in and above the HARP (High Amplitude Reflection Package) area, which is interpreted as an area of coarser grained sediment.

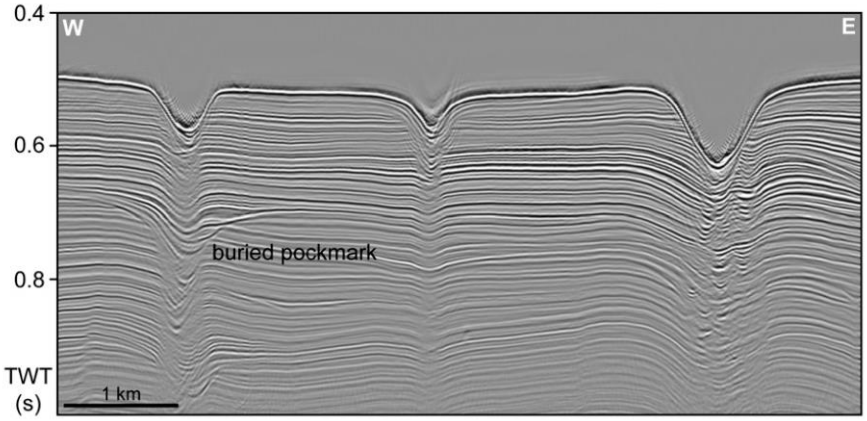

Fig. 9. MCS section through Category 3 structures showing downbending of layers below the craters, and a buried pockmark.

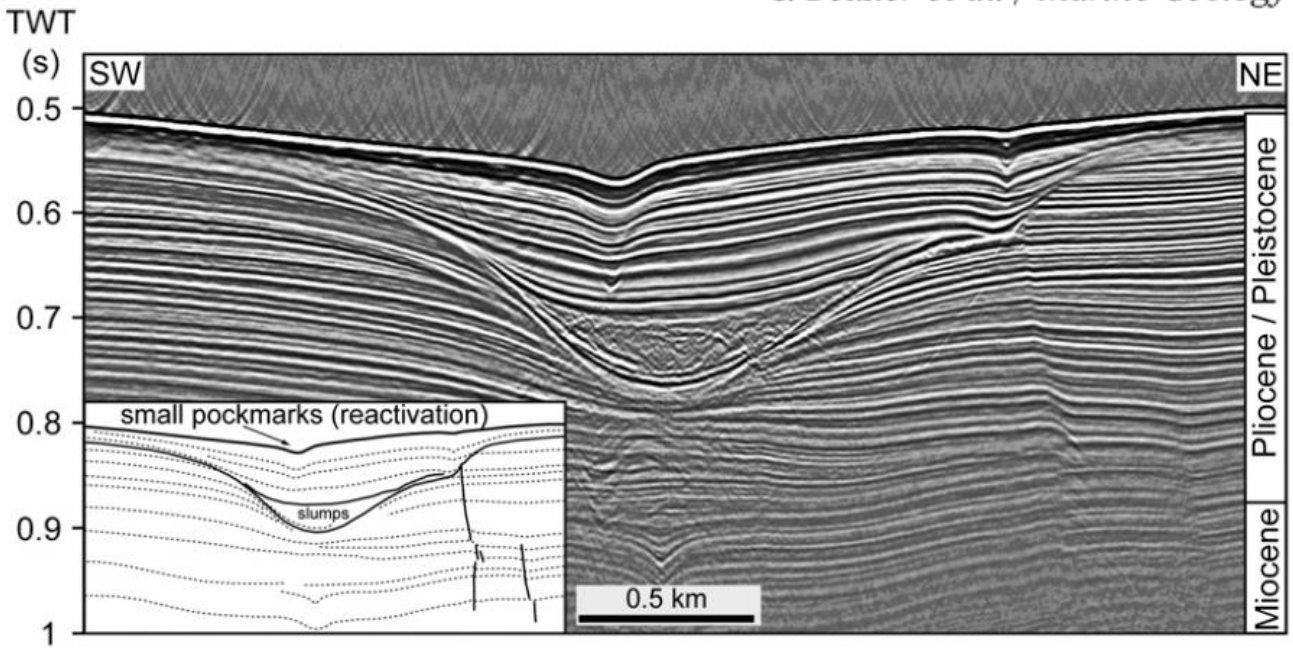

Fig. 11. MCS section through a Category 5 structure. Note wedging out of sediment fill, which is a result of the bottom current activity in the Inner Sea.

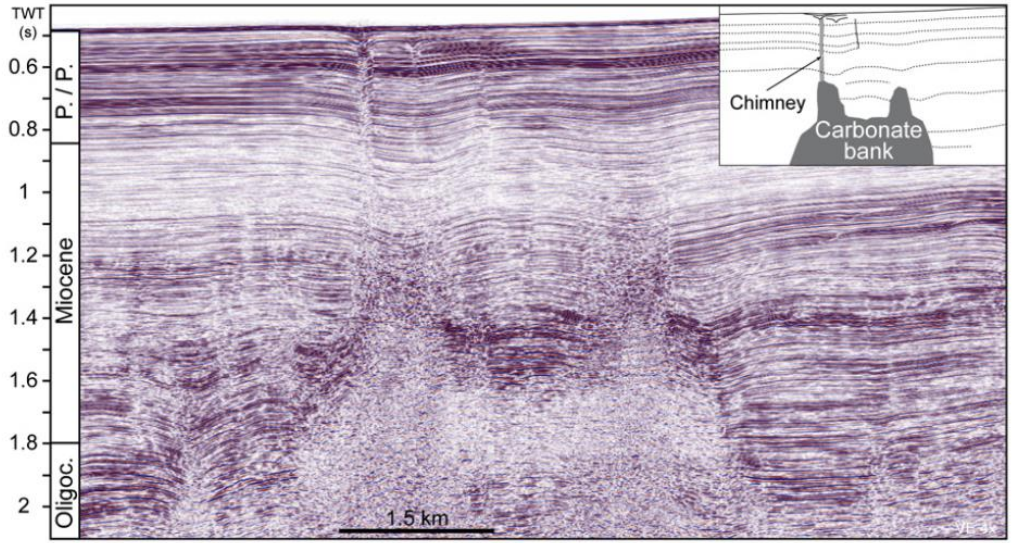

Fig. 15. MCS section showing the deeper subsurface of the Inner Sea, with a gas and fluid chimney rooted at the flank of an Oligocene–Miocene carbonate bank.

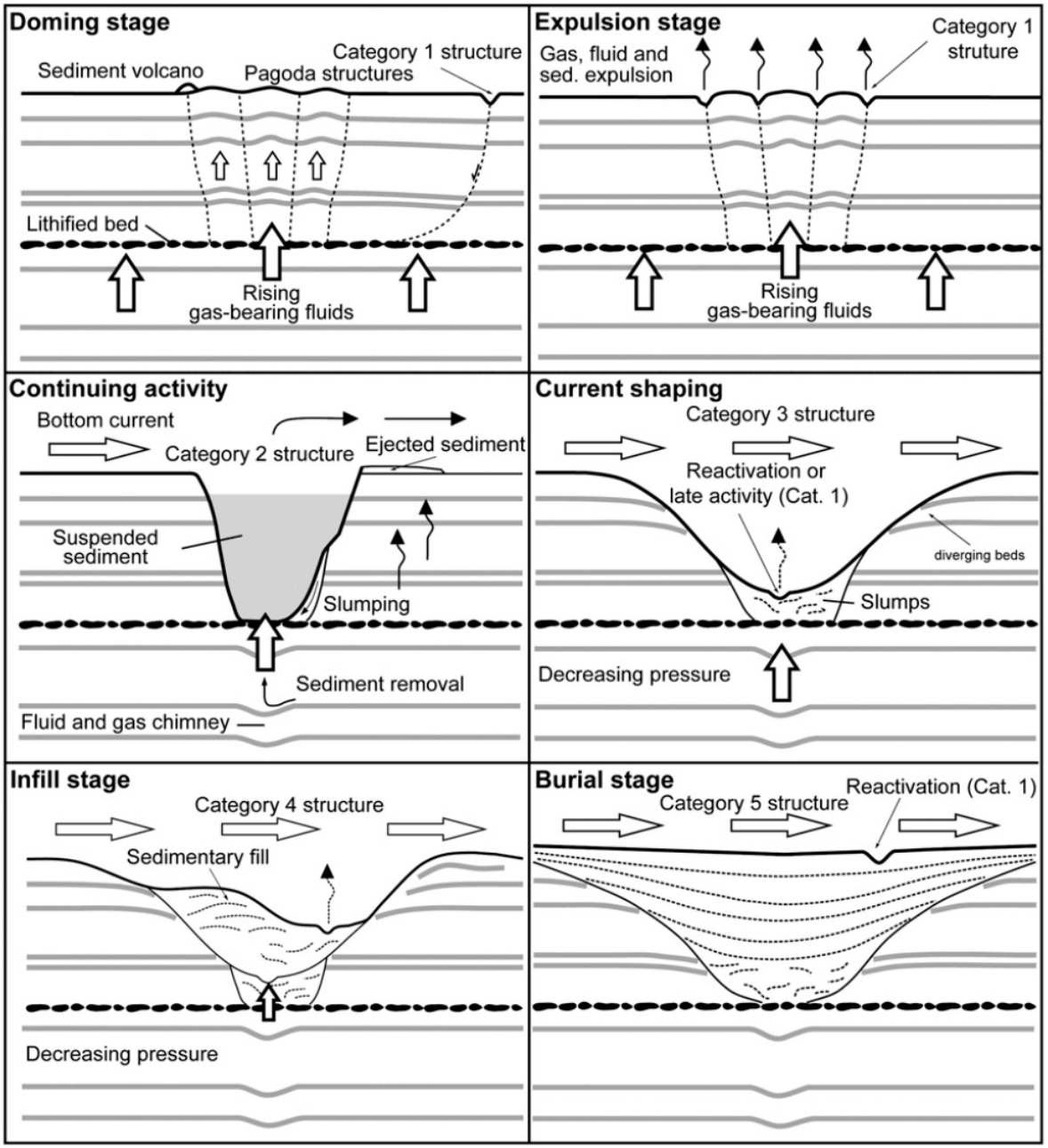

Fig. 17. Conceptual model for the different structures related to gas and fluid migration and venting in the Inner Sea. See text for explanation.

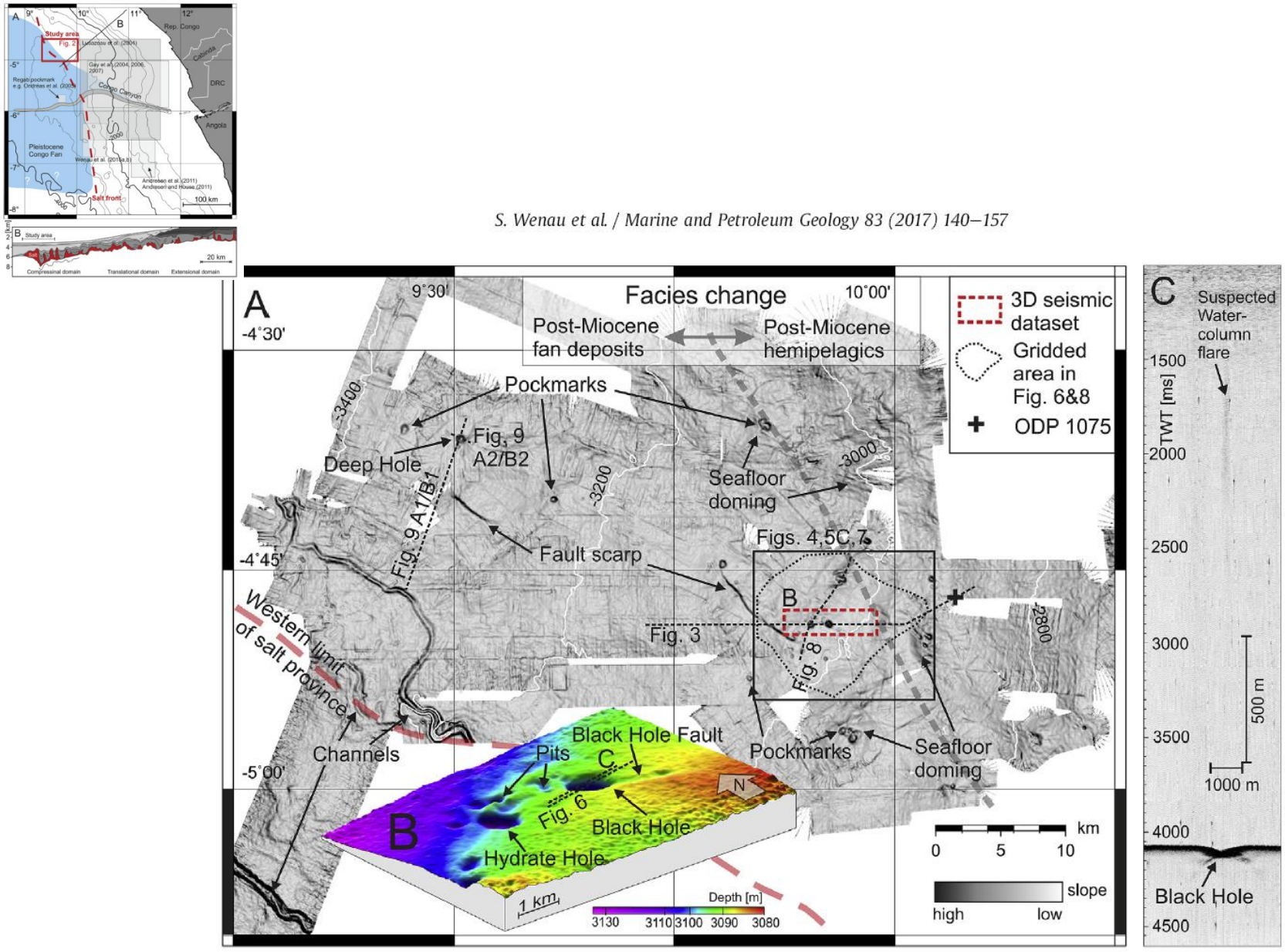

Fig. 2. A: Slope shaded map of the study area. For location see Fig. 1. Seafloor doming and pockmarks are prominent in the eastern part of the study area. Fault scarps are locally associated with seepage features. The dashed red line corresponds to the basinward limit of the salt basin (from Anka et al., 2009) B: High resolution bathymetric data around the 3D seismic dataset. Two prominent pockmarks are surrounded by secondary pits and seafloor fault scarps. C: Parasound 18 kHz water column echosounder profile over the Black Hole pockmark (B for location). A water column anomaly can be observed between 1500 and 2500 ms TWT above the seafloor pockmark, representing rising gas bubbles. (For interpretation of the references to colour in this figure legend, the reader is referred to the web version of this article.)

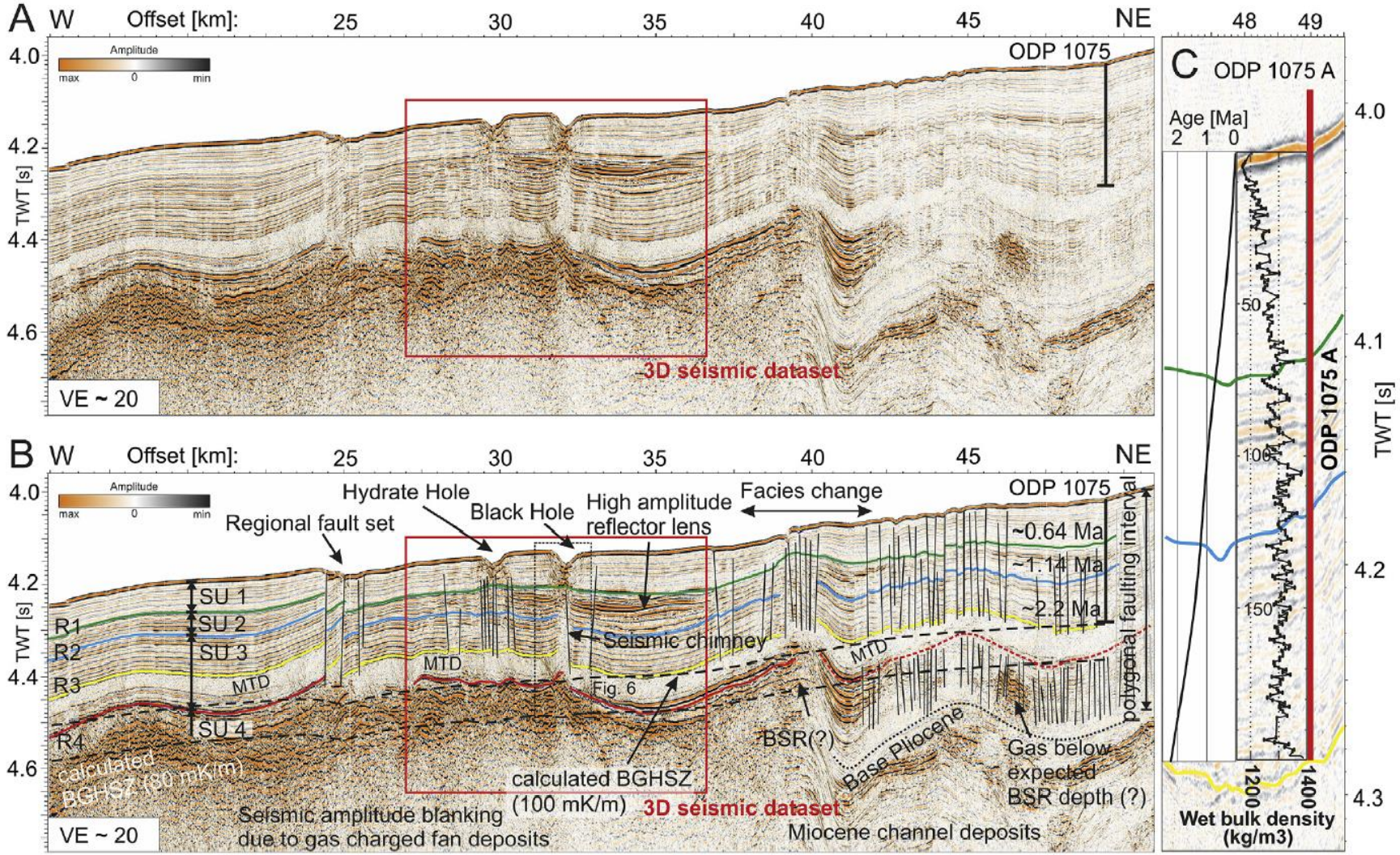

Fig. 3. A: Uninterpreted regional 2D seismic line through the study area. For location see Fig. 2A. B: Interpreted seismic line. The two pockmark features within the 3D seismic dataset are underlain by faults connecting gas charged fan deposits of Seismic Unit 4 to the seafloor. Note the transition in sedimentary facies towards the east from fan deposits and undisturbed hemipelagic sediments to polygonally faulted hemipelagic sediments at Offset 40 km. Reflector ages are inferred from by correlation with ODP Site 1075. B: Close-up of ODP Site 1075 showing the age model of ODP Hole 1075 A, the measured wet bulk density and correlated reflector ages.

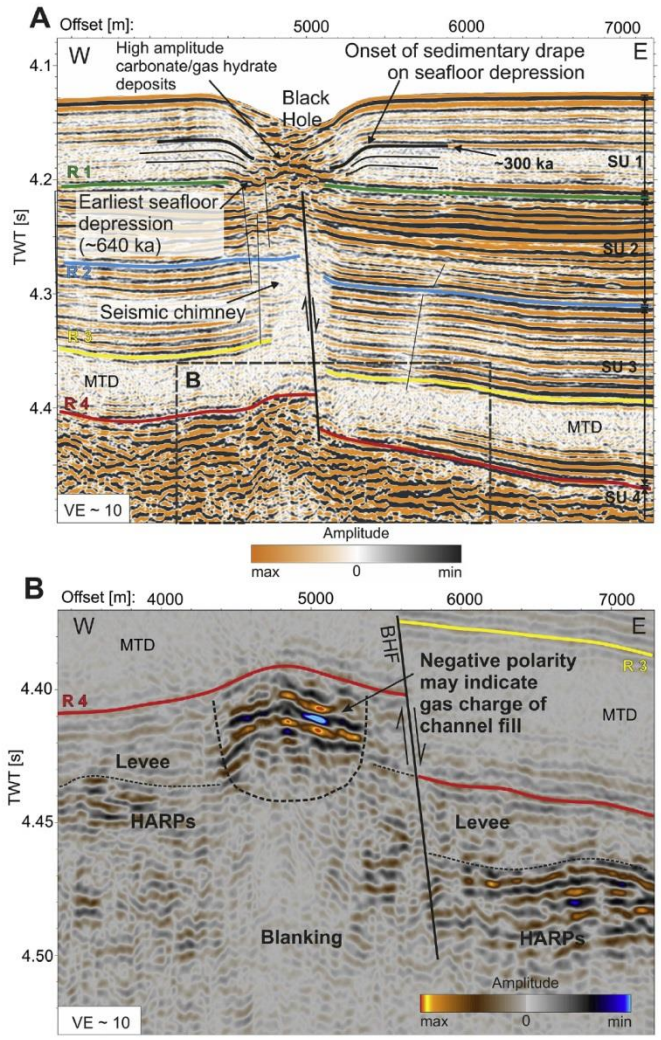

Fig. 6. A) Multichannel seismic line across the Black Hole pockmark. See Fig. 2B for location. A prominent fault connects a channel in Pliocene deposits and the seafloor. The onset o seepage at 640 kyr is suggested by reflection patterns in Seismic Unit 1. B) Multichannel seismic line of the Pliocene channel underlying Black Hole. Negative polarity reflections i the channel fill may indicate gas charging. BHF = Black Hole Fault.

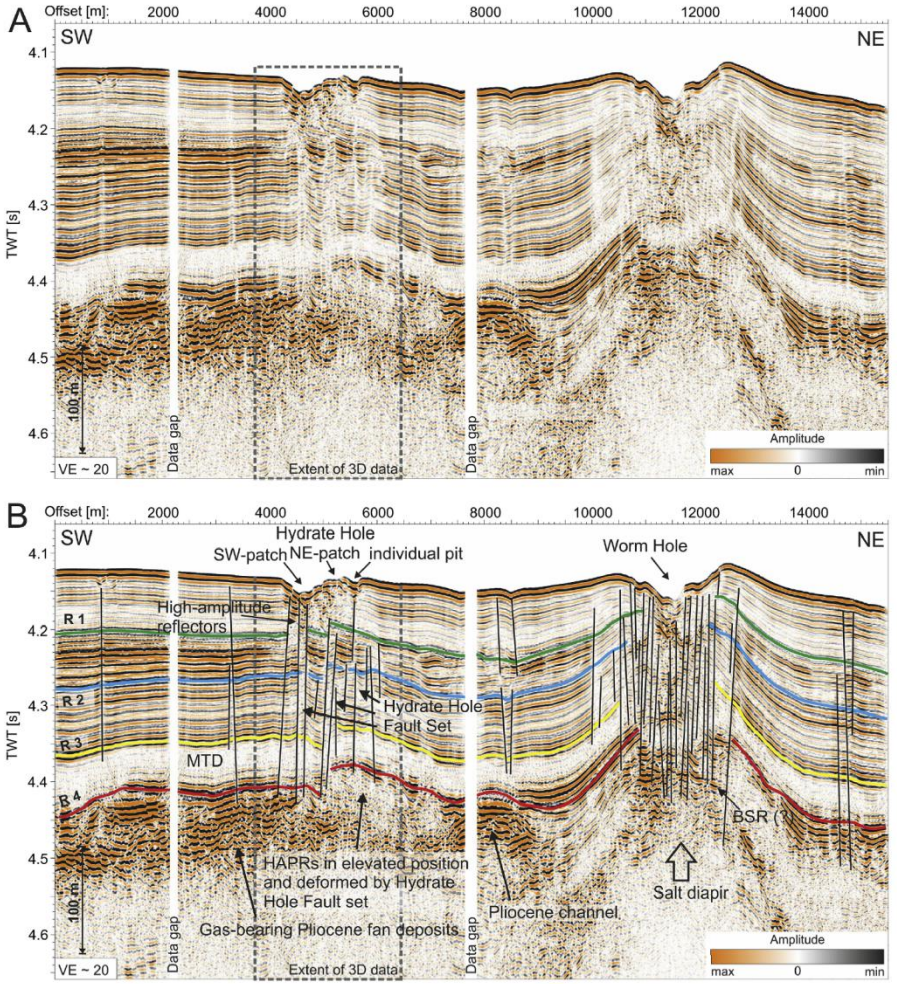

Fig. 8. Multichannel seismic SW-NE profile across Hydrate Hole and Worm Hole pockmarks. For location see Fig. 2A. A: Uninterpreted seismic line. B: Interpreted profile. The Hydrate Hole Fault set underlies the seepage features at the seafloor. Numerous faults form pathways for gas from Pliocene fan deposits, leading to the development of two individual seafloor seepage locations and also secondary pits. The NE-patch constitutes the currently active seep site. Worm Hole is situated on a salt diapiric structure inferred from the tilted sedimentary flanks and seafloor doming. A BSR is interpreted at the summit of the diapiric structure probably formed due to the focusing of gas migration in the tilted sedimentary flanks and illustrates the accumulation of gas that may support seafloor seepage. The Pliocene channel structure underlying Black Hole (Fig. 5B) can be seen in its northward continuation in the center of the profile.

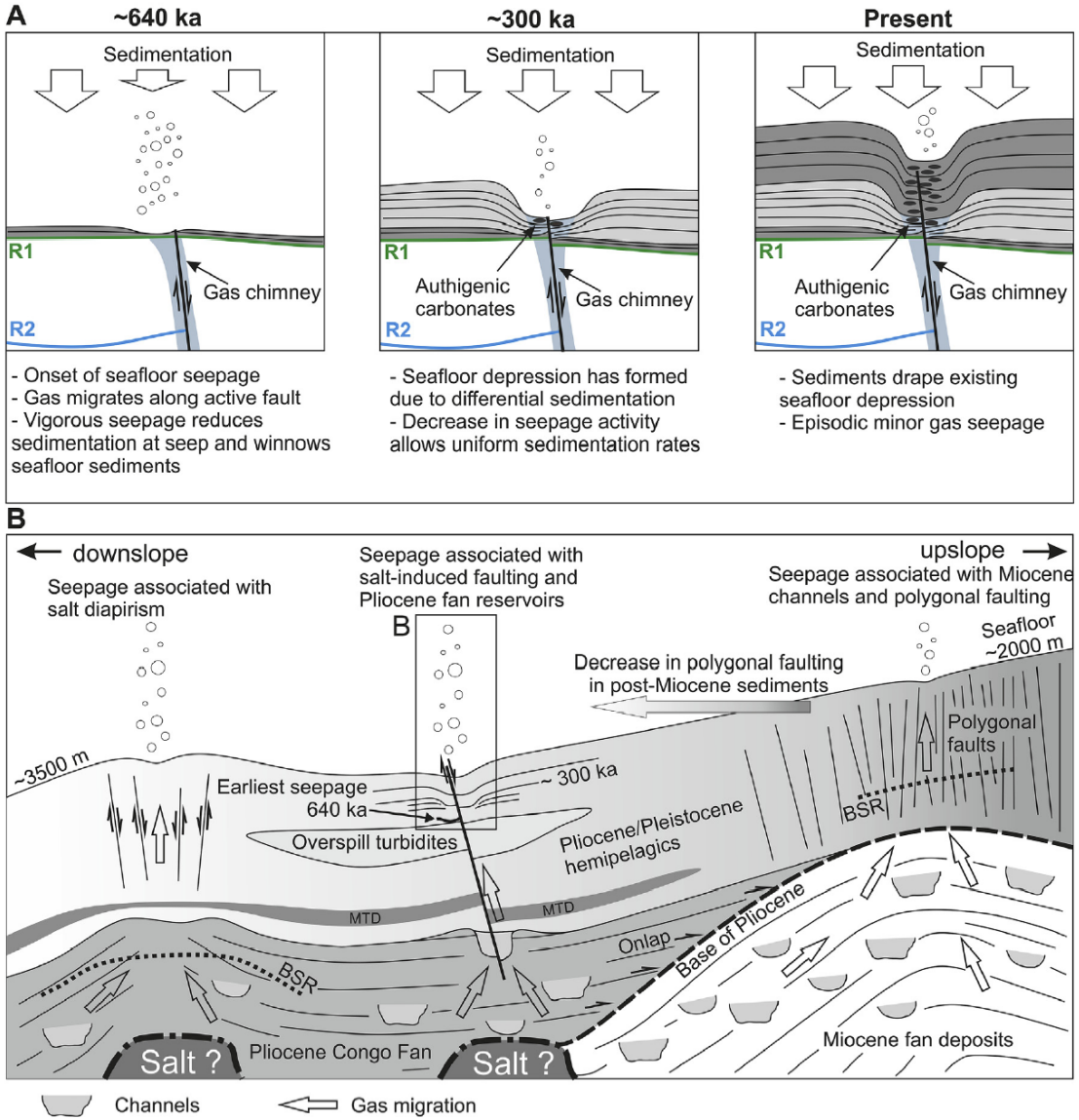

Fig. 10. A: Sketch of the formation history of observed giant pockmarks in the study area. The onset of seepage at 640 kyr along a salt-induced fault led to reduced sedimentation at the seepage site. A reduction in seepage activity at 300 kyr led to increased sedimentation over the pockmark, draping the existing seafloor depression. B: Scheme of the geological setting of gas migration and seafloor seepage in the deep water northern Lower Congo Basin. Miocene channel deposits act as reservoirs for rising gas. Seal breaching of overlying hemipelagic deposits is achieved via polygonal faults in the upslope regions of the LCB (Gay et al., 2007; Andresen et al., 2011). Gas of shallow microbial origin accumulates within high-porosity channel-fills at the BGHSZ in our study area. Seepage is promoted by salt-induced faulting that creates pathways from Pliocene Fan deposits to the seafloor in the absence of polygonal faults in the vicinity of the Pliocene/Pleistocene Congo fan. Similarly, large scale sedimentary deformation by salt diapirism on the lower slope leads to the focusing of gas towards the seafloor from the Pliocene fan deposits and facilitates the breaching of the hemipelagic seal. MTD - Mass transport deposit, BSR - Bottom simulating reflector.

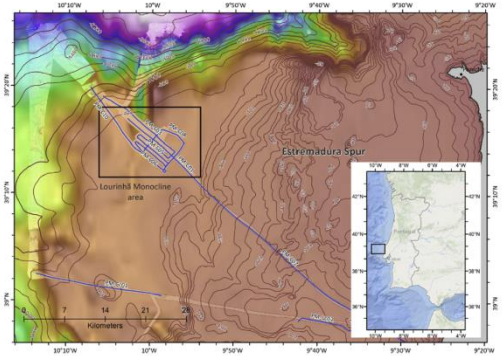

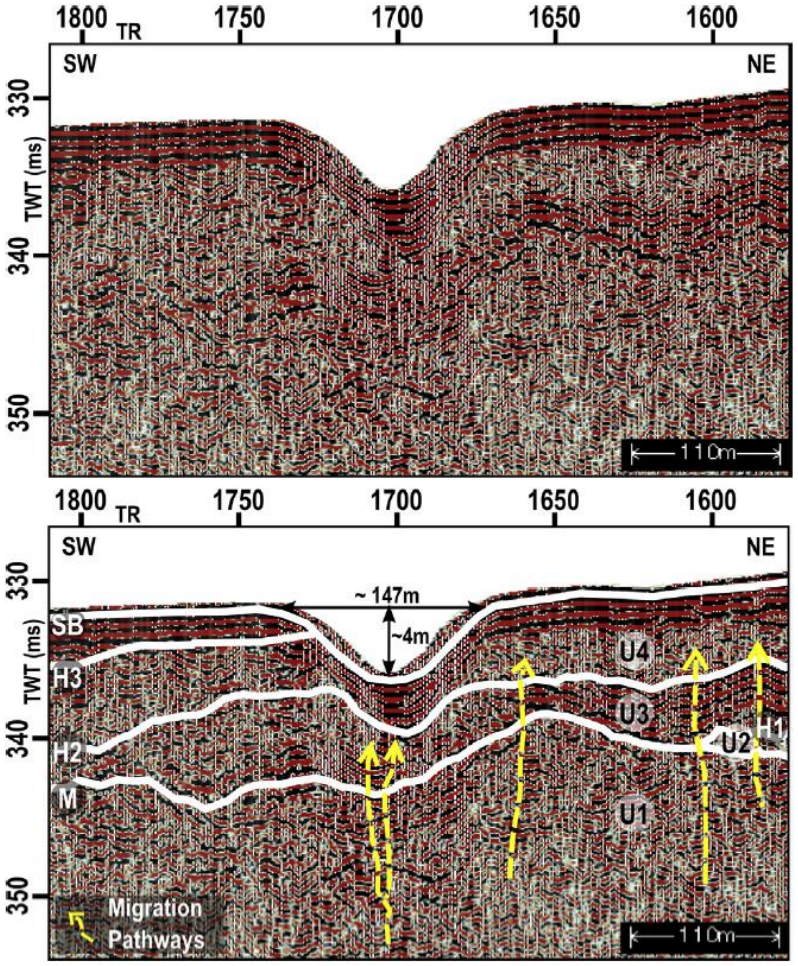

Fig. 6. Detail of seismic profile PM-C09 showing a pockmark at the seabed (Fig. 2 for location).

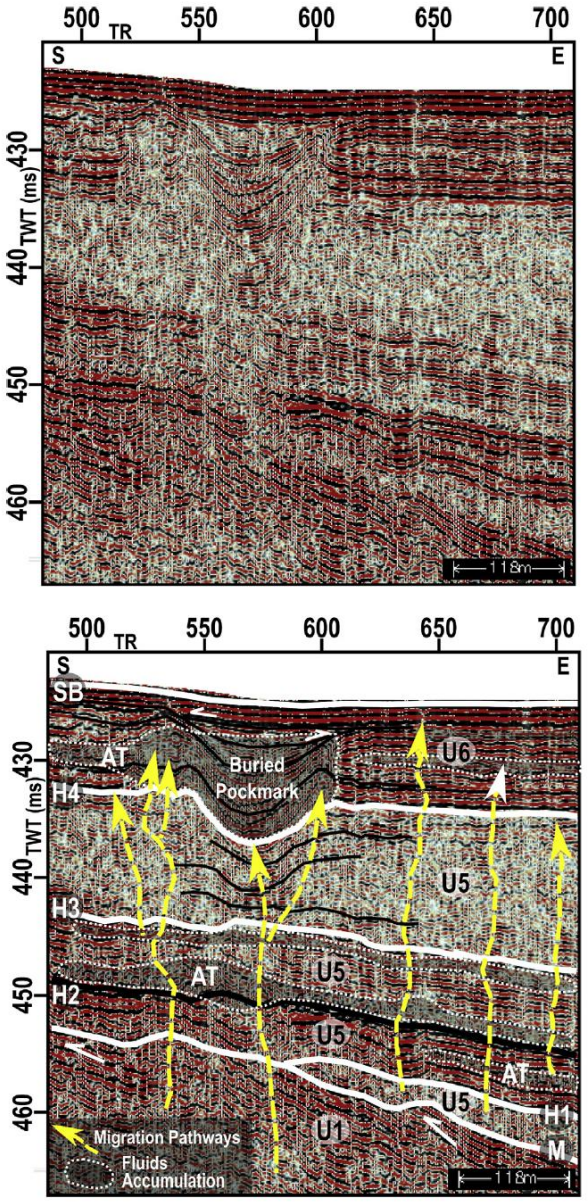

Fig. 7. Detail of seismic profile PM-C07 showing a buried pockmark and sub-seafloor evidences for fluid migration. Layers with AT are interpreted as fluids reservoirs (Fig. 2 for location).

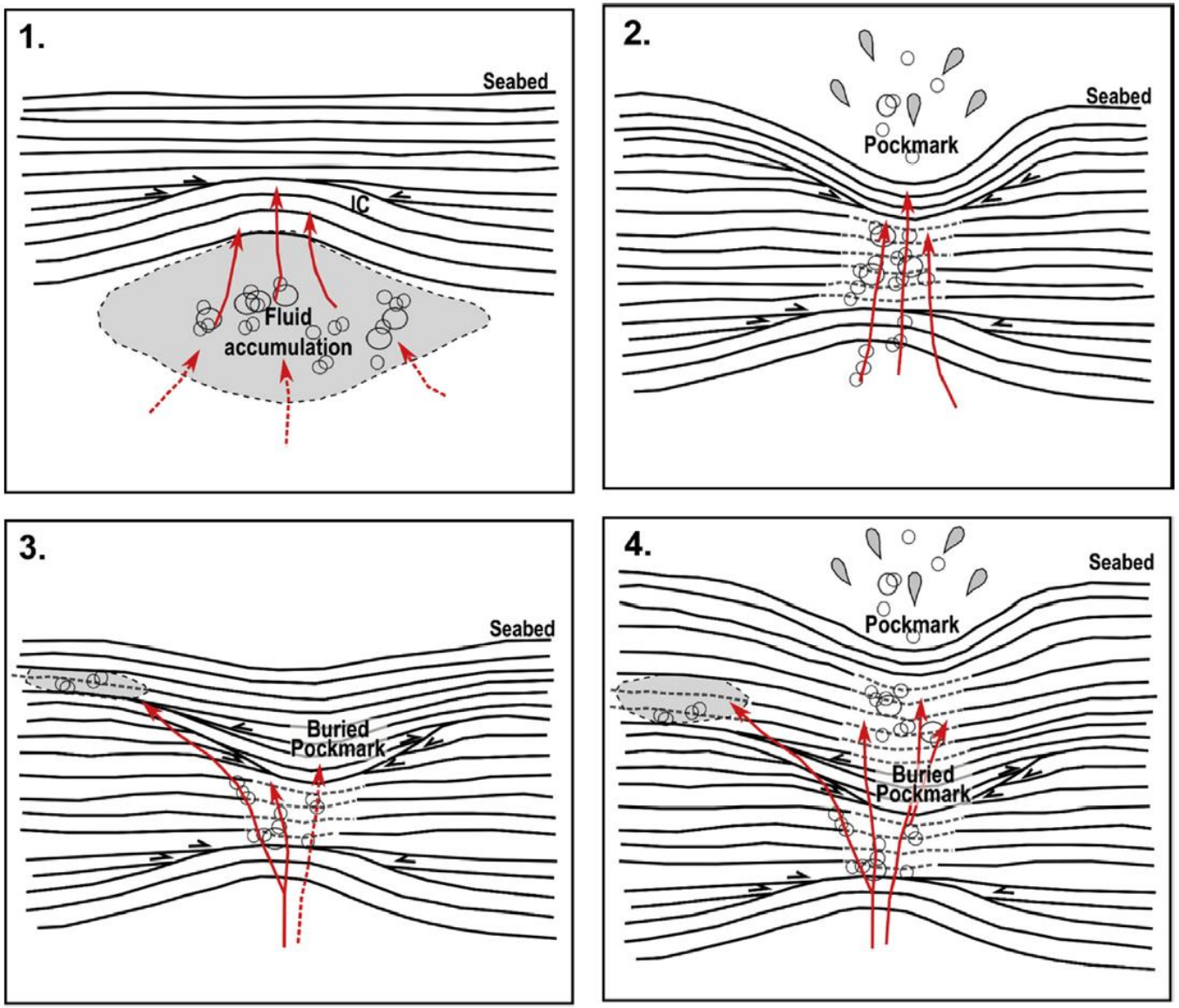

Fig. 10. Seepage evolution hypothesis (see text for discussion, 5.3.1). Red arrows: migration pathways; Red dashed arrows: possible migration pathways; Circles and drops: fluid; Dashed grey lines: acoustically disturbed reflection; Black arrows: onlap terminations. (For interpretation of the references to colour in this figure legend, the reader is referred to the web version of this article.)

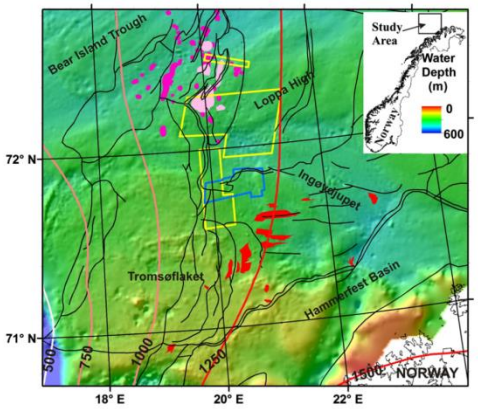

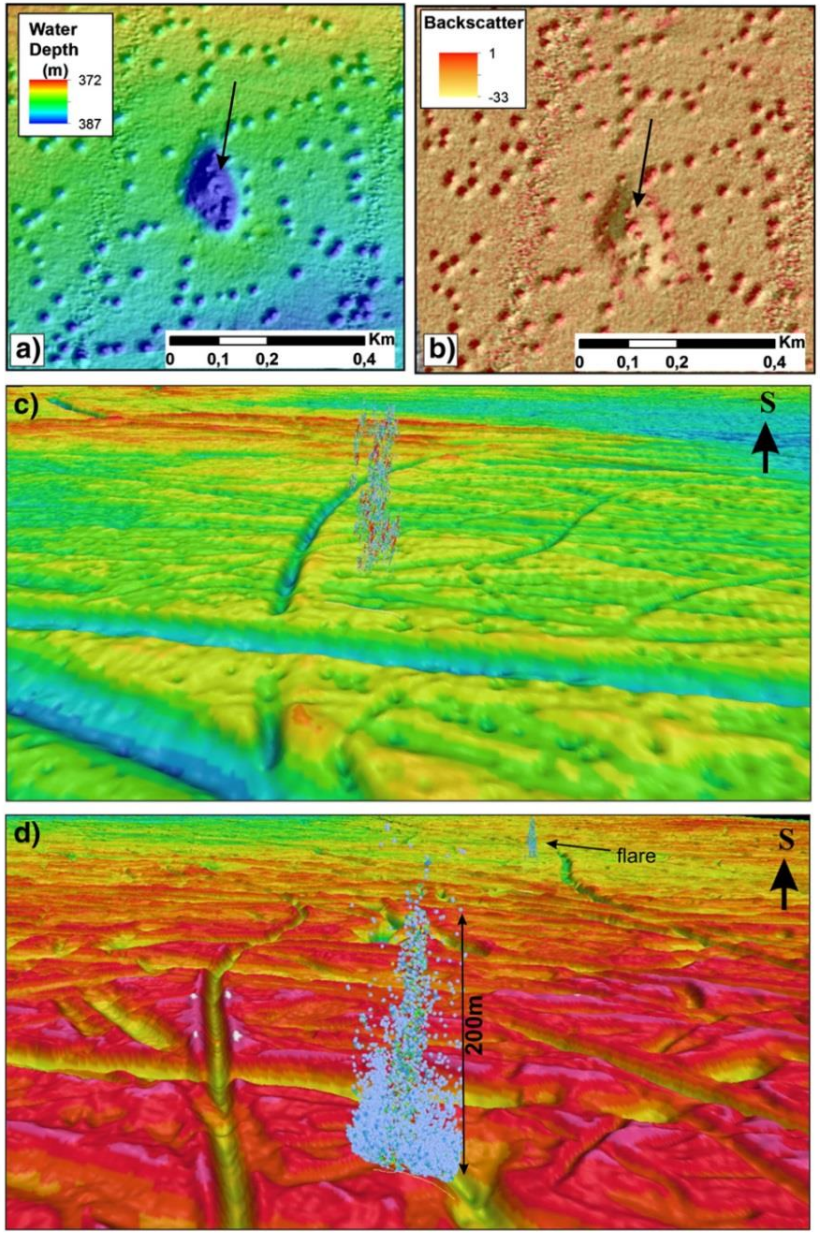

Fig. 3. a) Bathymetry and b) backscatter datasets showing the structure and backscatter properties of pockmarks and depressions. Notice the occurrence of pockmarks within depressions. Gas flares from c) pockmark area and d) non pockmark area shown on shaded relief bathymetry. Notice that the flares occur from iceberg plough marks. See Fig. 2 for location.

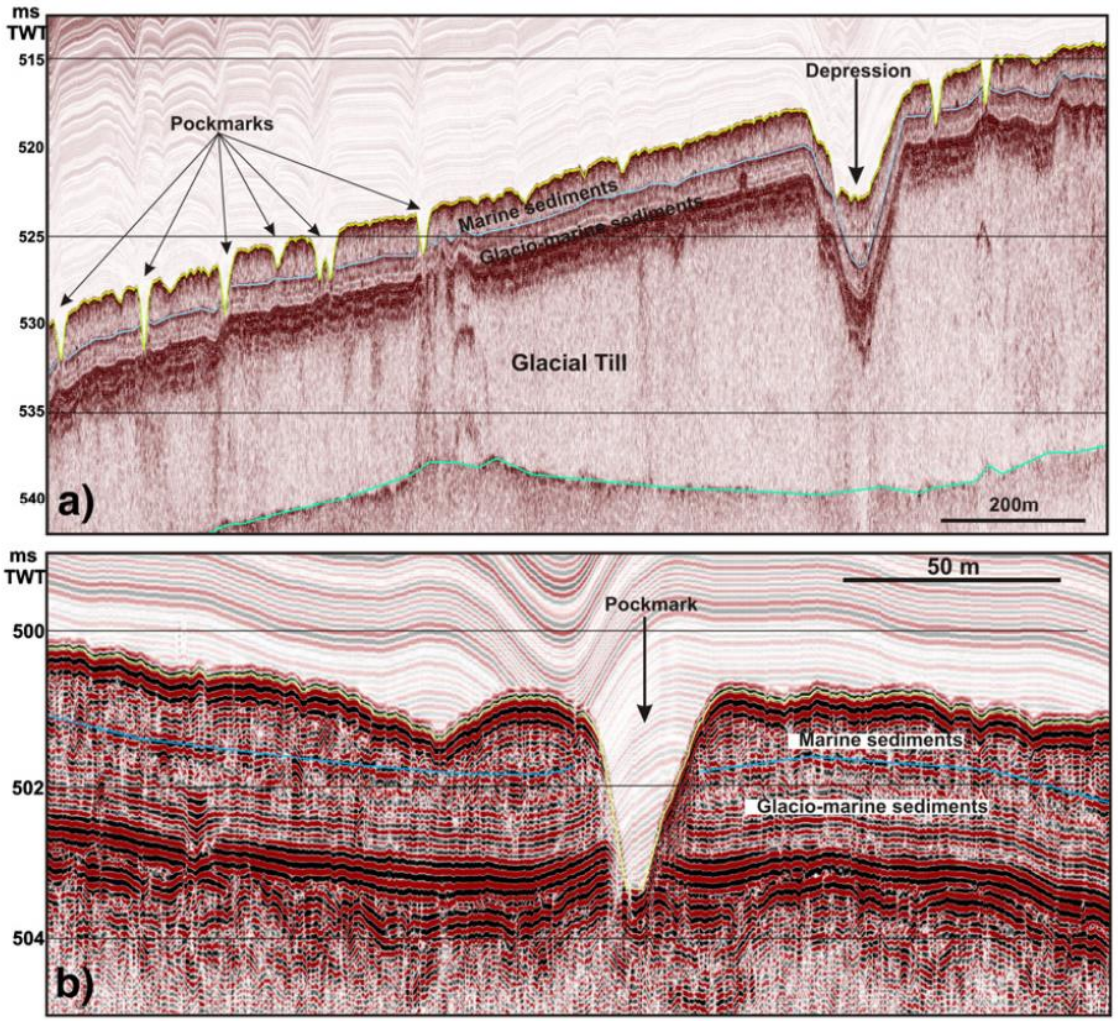

Fig. 5. a) High resolution SBP line across the pockmark area showing subsurface sedimentary structure of the pockmarks and depressions. Notice that the depression is infilled with marine and glaciomarine sediments while pockmarks look fresh with very little marine sediments. b) High resolution SBP image of pockmark showing that they have very little marine sediments deposited. The pockmark is cutting across the marine–glaciomarine boundary (blue line) indicating that they formed after the deposition of glaciomarine sediments. See Fig. 2 for location.

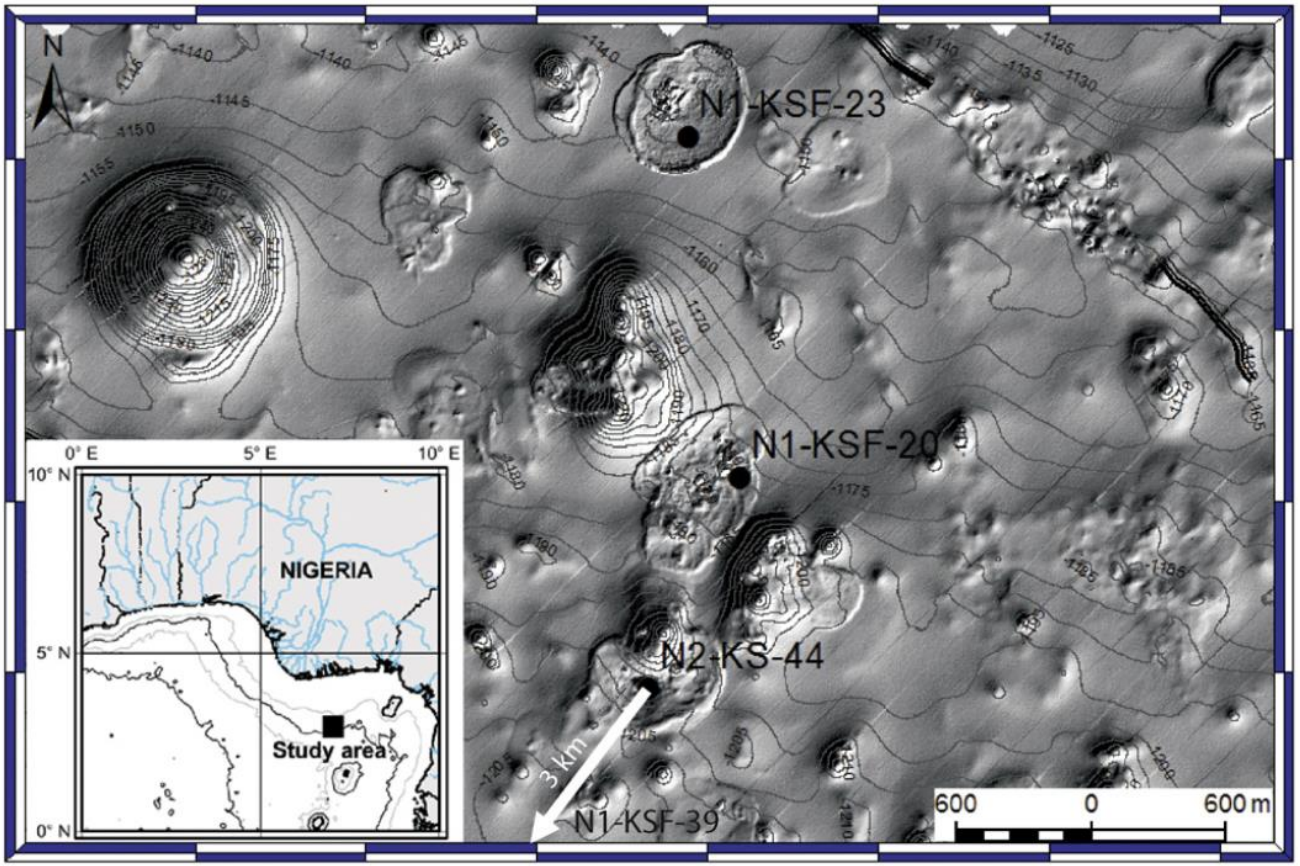

Fig. 1. Bathymetric map of the studied area with position of the studied cores. This area corresponds to the collapsed summit of an anticline, which is delimited by two deep-rooted normal faults. Note that core N1-KSF-39 is located about 3 km south-west of core N2-KS-44.

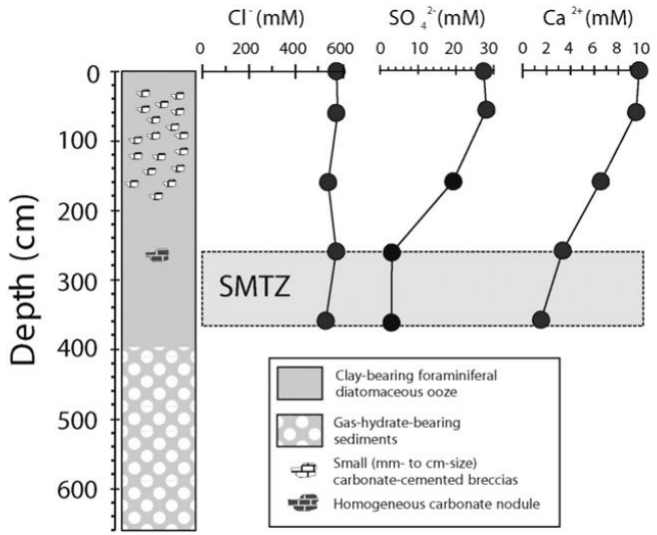

Fig. 2. Lithological description of core N2-KS-44 and corresponding pore-water sulphate, calcium and chloride profiles. Analytical uncertainties are within the size of the symbols. Note that original photographs of the studied carbonate concretions can be found in Bayon et al. (2007).

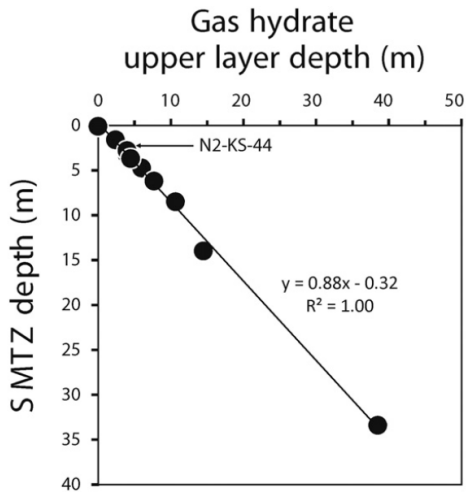

Fig. 7. Relationship between the depth of the sulphate-methane transition zone (SMTZ) and the depth of occurrence of gas hydrate nodules in the study area. The plot was constructed using data for core N2-KS-44 (this study) and previously published data (Rongemaille, 2011; Ruffine et al., 2013; Sultan et al., 2014; de Prunelé et al., 2015).

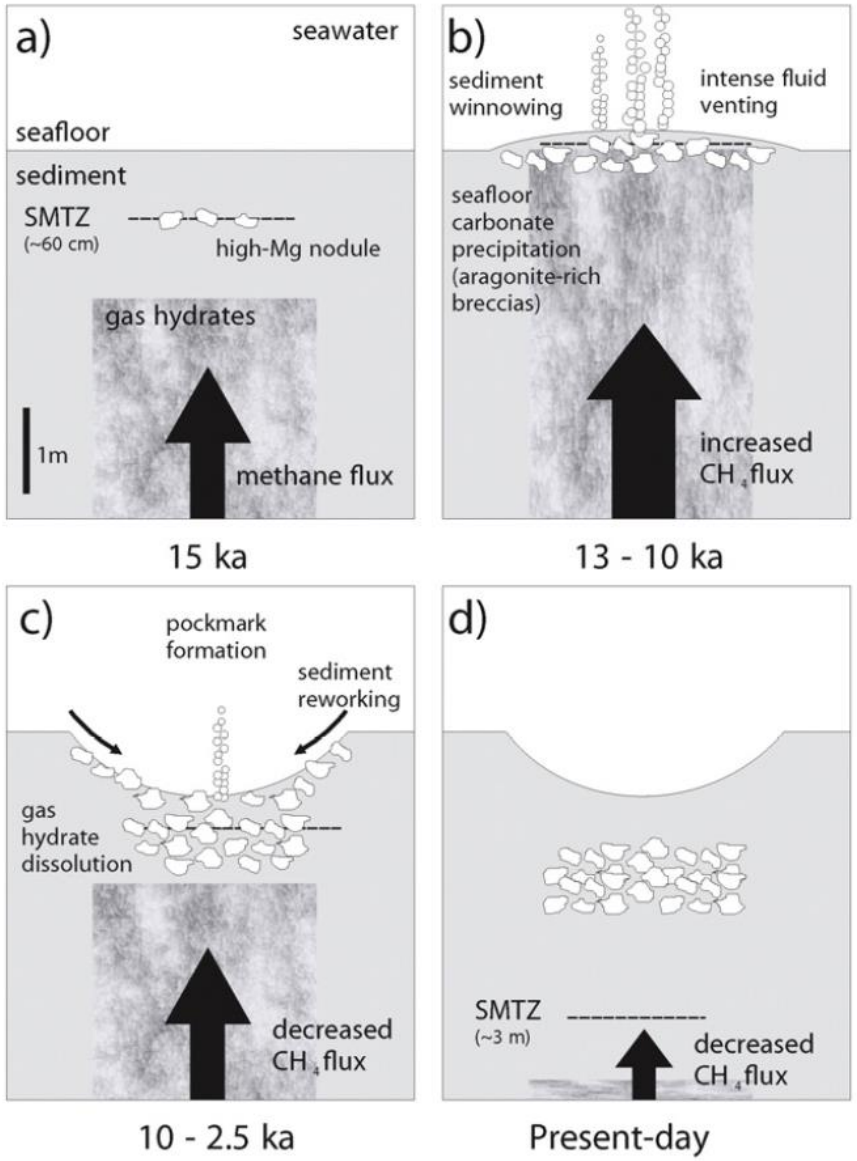

Fig. 9. (a to d) Conceptual model for gas hydrate dynamics and pockmark evolution at the studied site (see text for details).

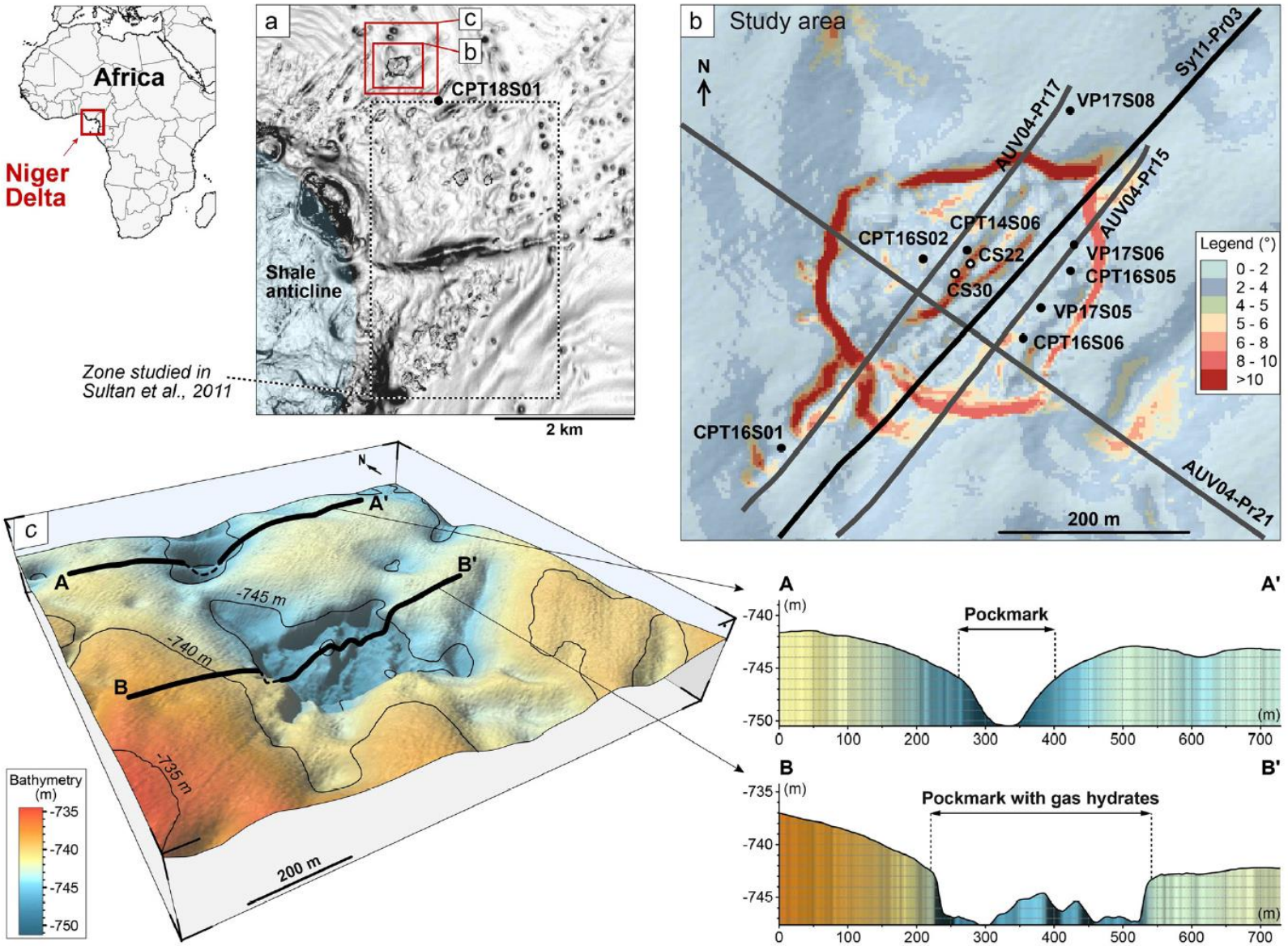

Fig. 1. a: Location maps of the area of interest presenting the seafloor morphology with the dip map derived from the bathymetry (horizontal resolution: 3 m). We study a small area located at the north of the area studied in Sultan et al. (2011). b: The location of all data used in this study (HR seismic profiles, cores and geotechnical data) is projected on the seafloor dip map. c: The 3D view of the area of interest shows two types of seafloor deformations and the location of two bathymetric profiles. The bathymetric profiles AA′ and BB′ correspond, respectively, to a Type-1 pockmark and a Type-2 pockmark.

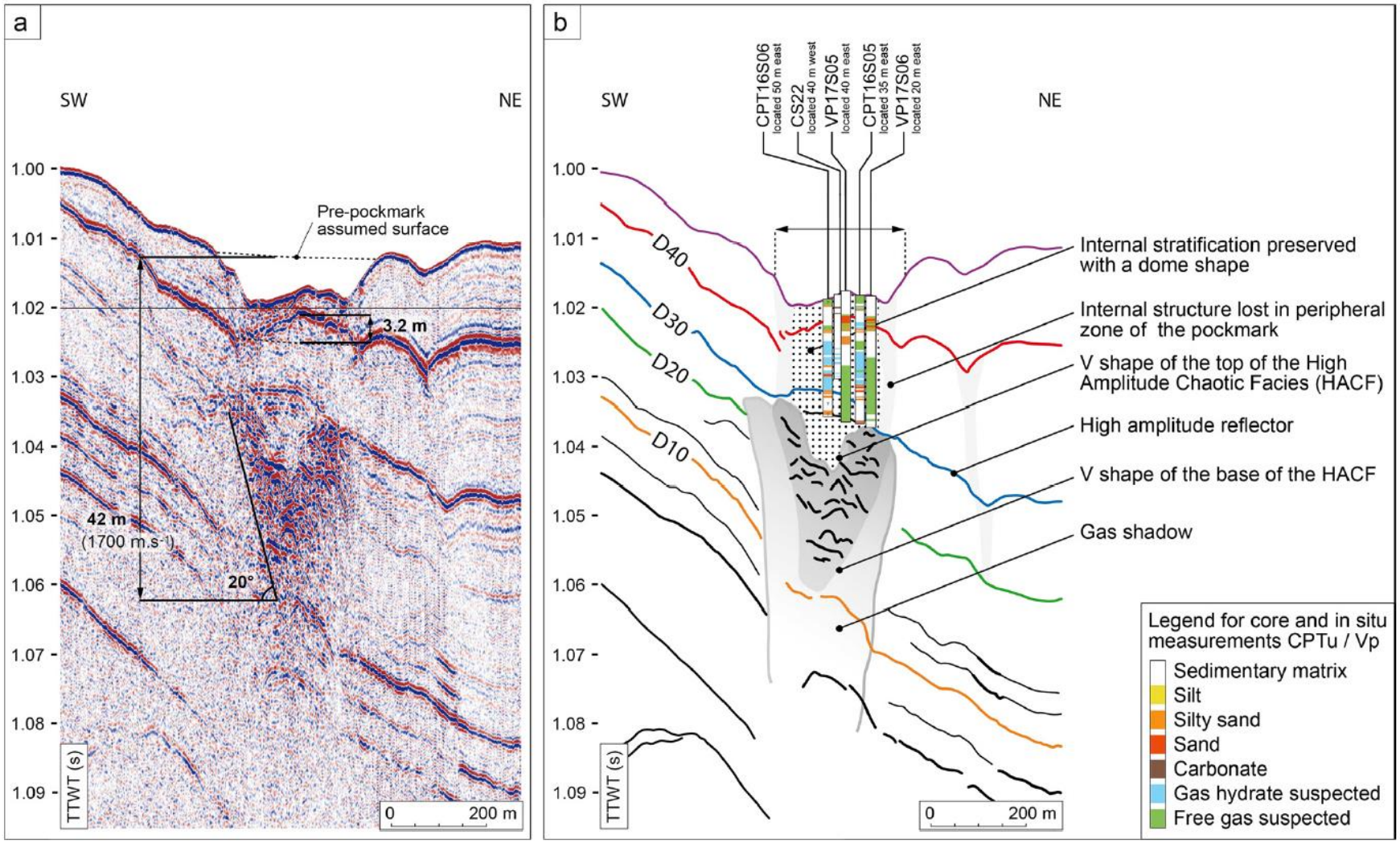

Fig. 3. 2D high resolution seismic profile (Sysif profile SY11-Pr03 – for location see Fig. 2) with its stratigraphic interpretation showing the studied pockmark internal structure with the location and interpretation of in situ measurements and sedimentary cores. CPTu: Piezocone penetration testing and Vp: Velocity of the primary wave.

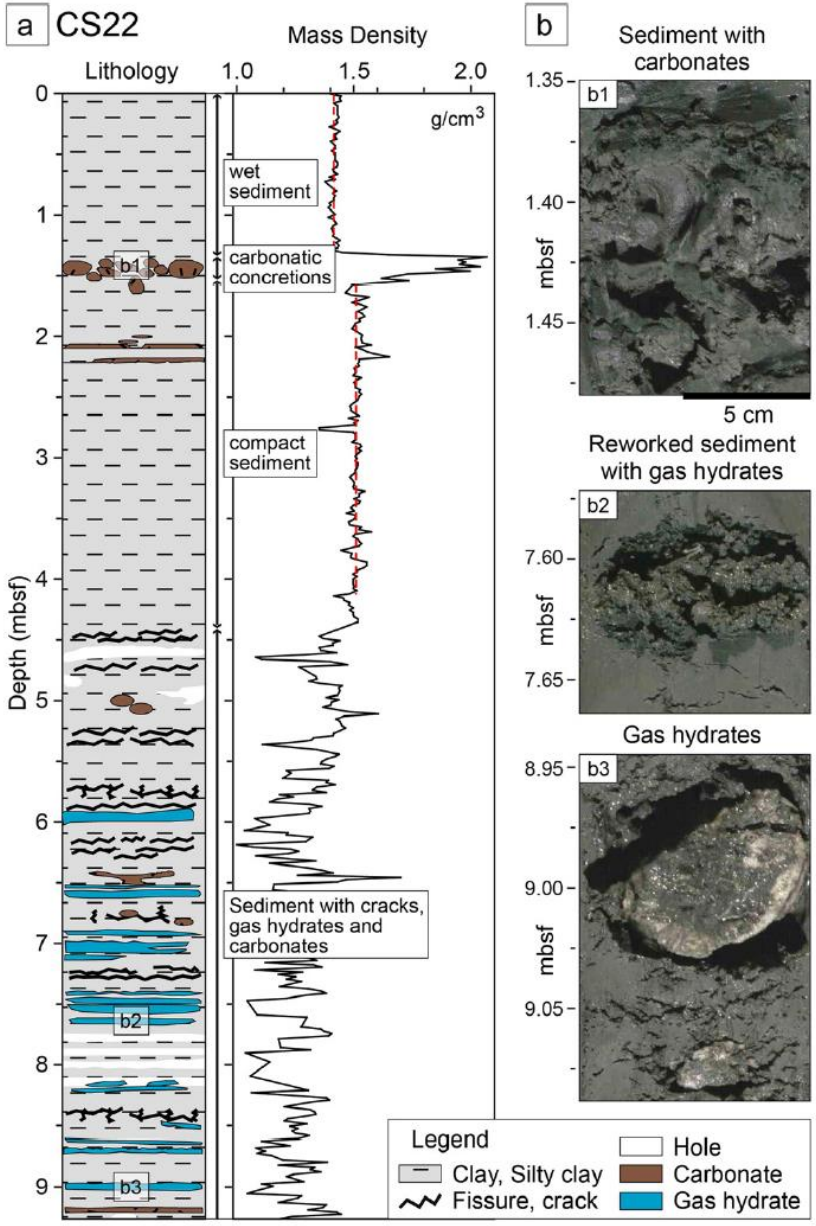

Fig. 4. Calypso core CS22 recovered from the central part of the pockmark, a: log and mass density values versus depth. b: Pictures of recovered carbonates and gas hydrates.

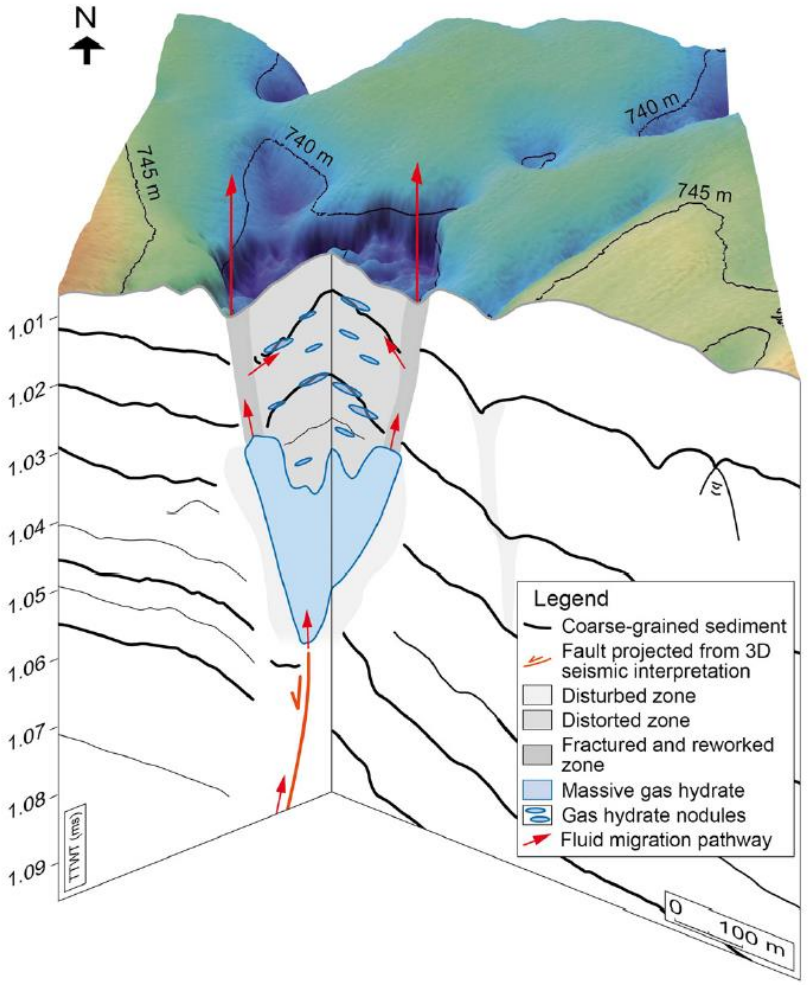

Fig. 5. 3D interpretative view of the pockmark reveals gas migration pathway from the major fault to the seafloor. The blue V shape corresponds to the presence of massive gas hydrate at the origin of the seafloor deformation/depression. Red arrows indicate possible fluid fluxes within the studied pockmark. (For interpretation of the references to color in this figure legend, the reader is referred to the web version of this article.)

major fault. The area affected by fluid activities is localized under the sub-surface sedimentary deformation marked by the pockmark.

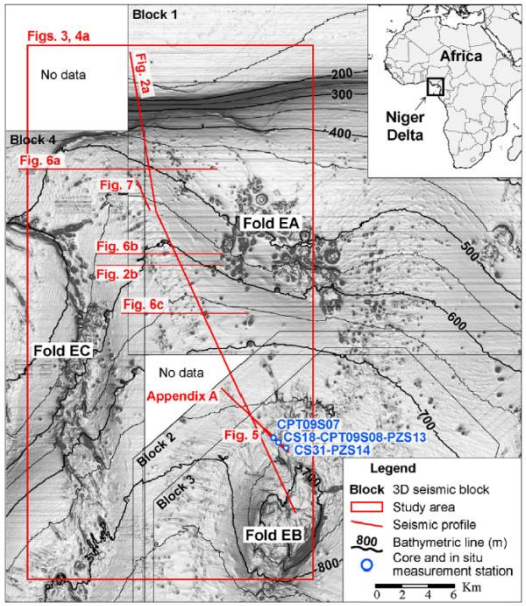

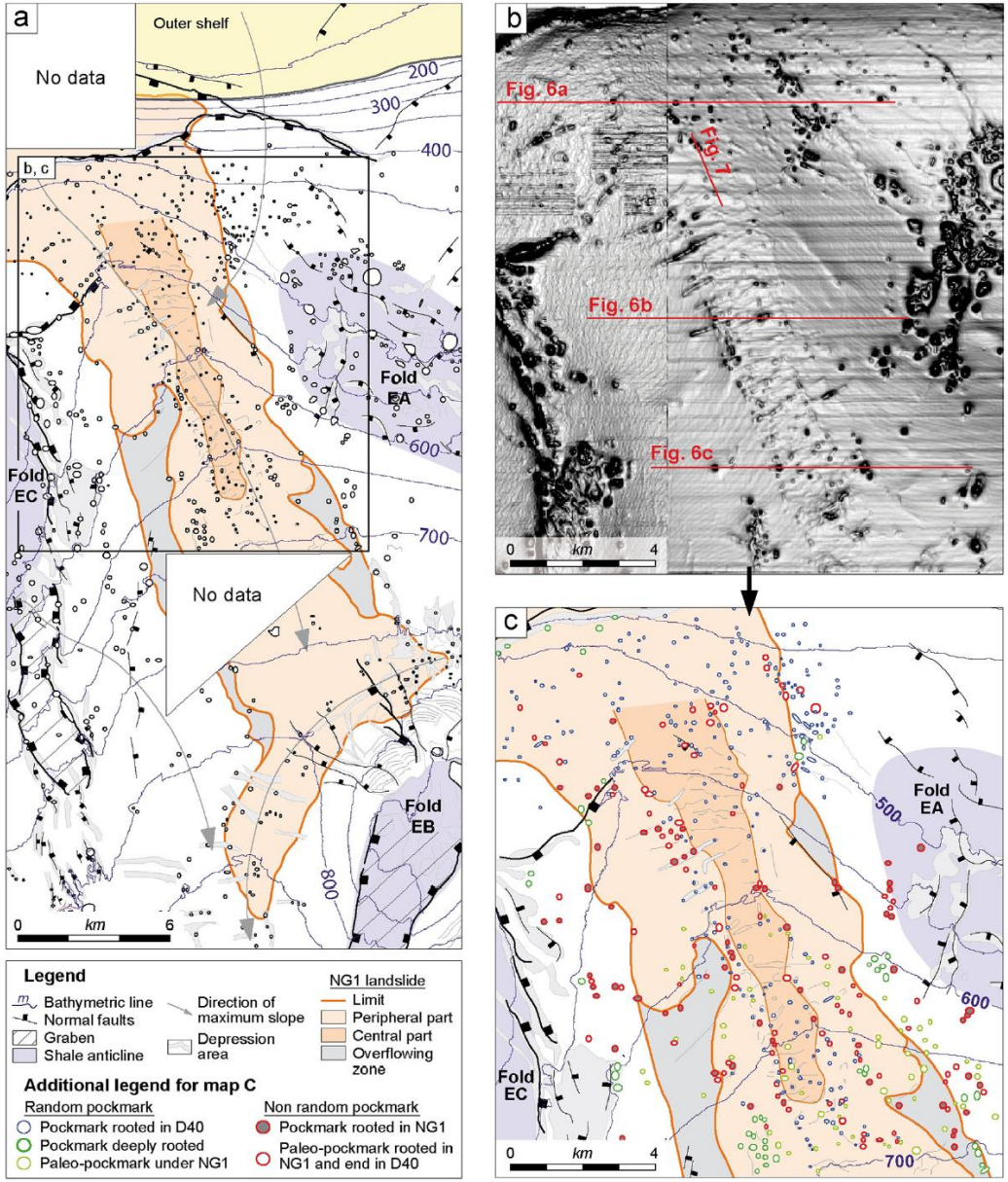

Fig. 4. (a) Geomorphologic map of NG1 landslide and surrounding area obtained from the interpretation of the bathymetric map and of the 3D seismic data. Faults affecting the seabed are in black, pockmarks in black and white, shale folds in gray and outer continental shelf in yellow. (b) Dip map of the study area with location of the following figures in red. (c) Geomorphologic map of the study area showing the different group of pockmarks described in the study area from the interpretation of 3D seismic data. The non-random pockmarks (in red) are rooted in the NG1 internal discontinuities, while the random pockmarks (in blue) are connected to D40 reflector and the random pockmarks (in green) are more deeply rooted. (For interpretation of the references to color in this figure legend, the reader is referred to the web version of this article.)

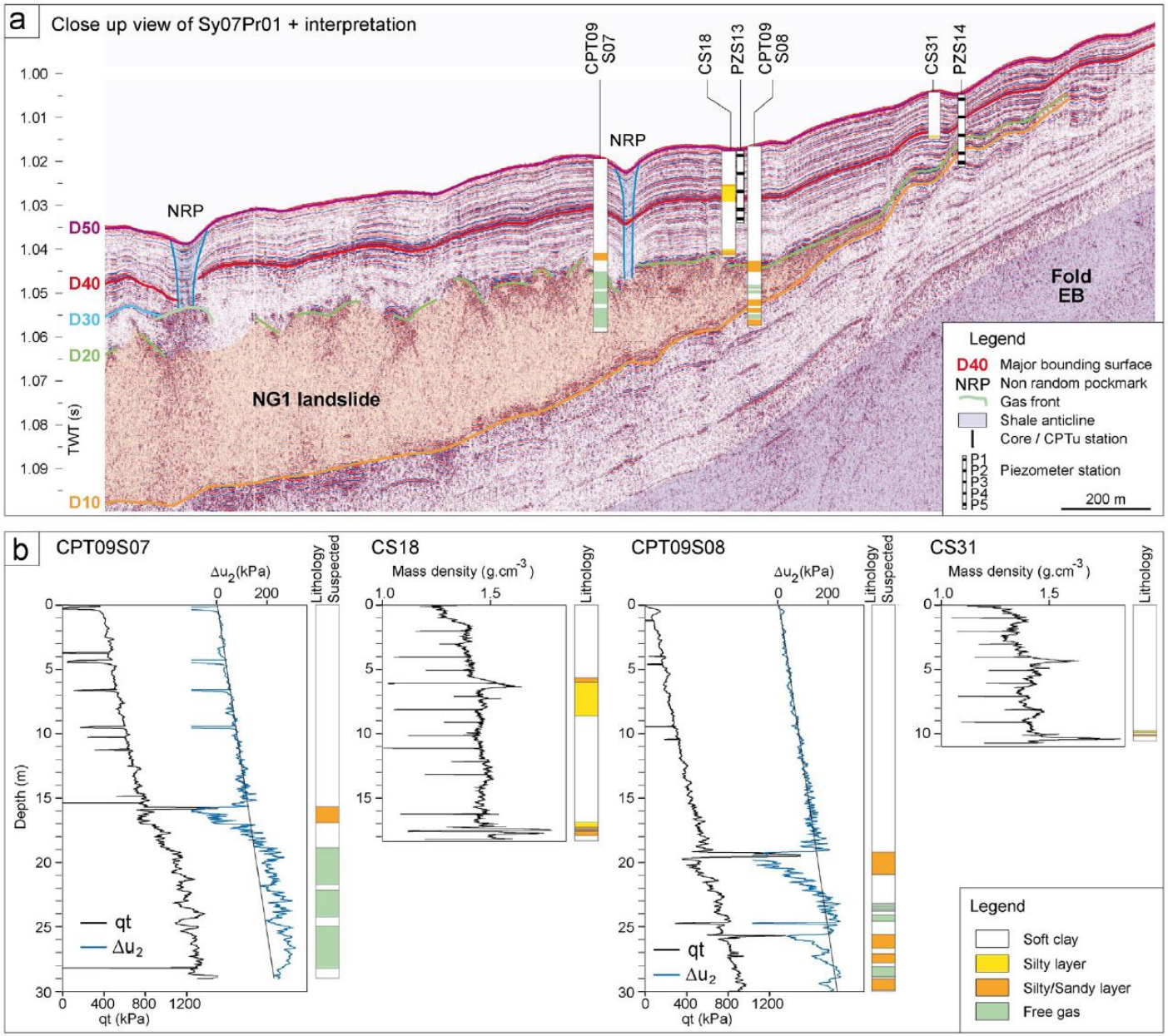

Fig. 5. (a) Close up view of the 2D HR seismic lines presented in Fig. S2 with interpreted piezocone and core data. NRP=Non-Random Pockmark. (b) Corrected cone resistance qt and excess pore pressure $\Delta u2$ versus depth from sites CPT09S07 and CPT09S08. Mass density values versus depth and lithology presented for cores CS18 and CS31. See text for details.

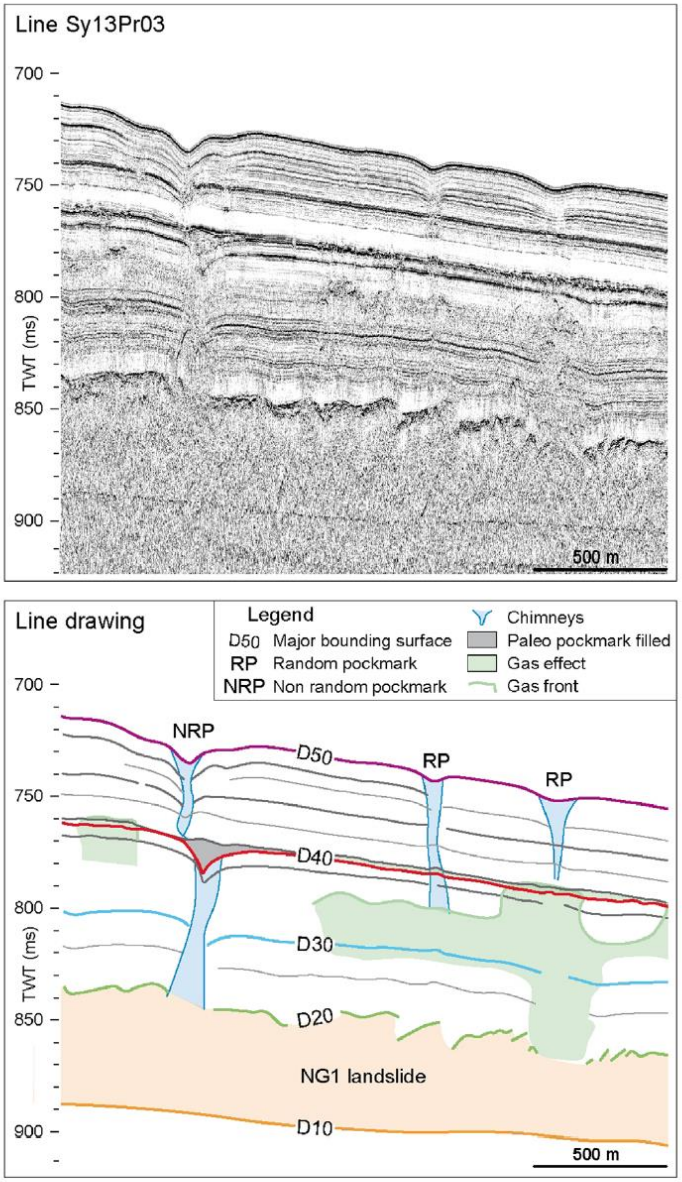

Fig. 7. 2D HR seismic lines acquired with the SYSIF system along the same track of the seismic line presented in Fig. 2, showing more details about the features described and the precise location of fluids within sediment.

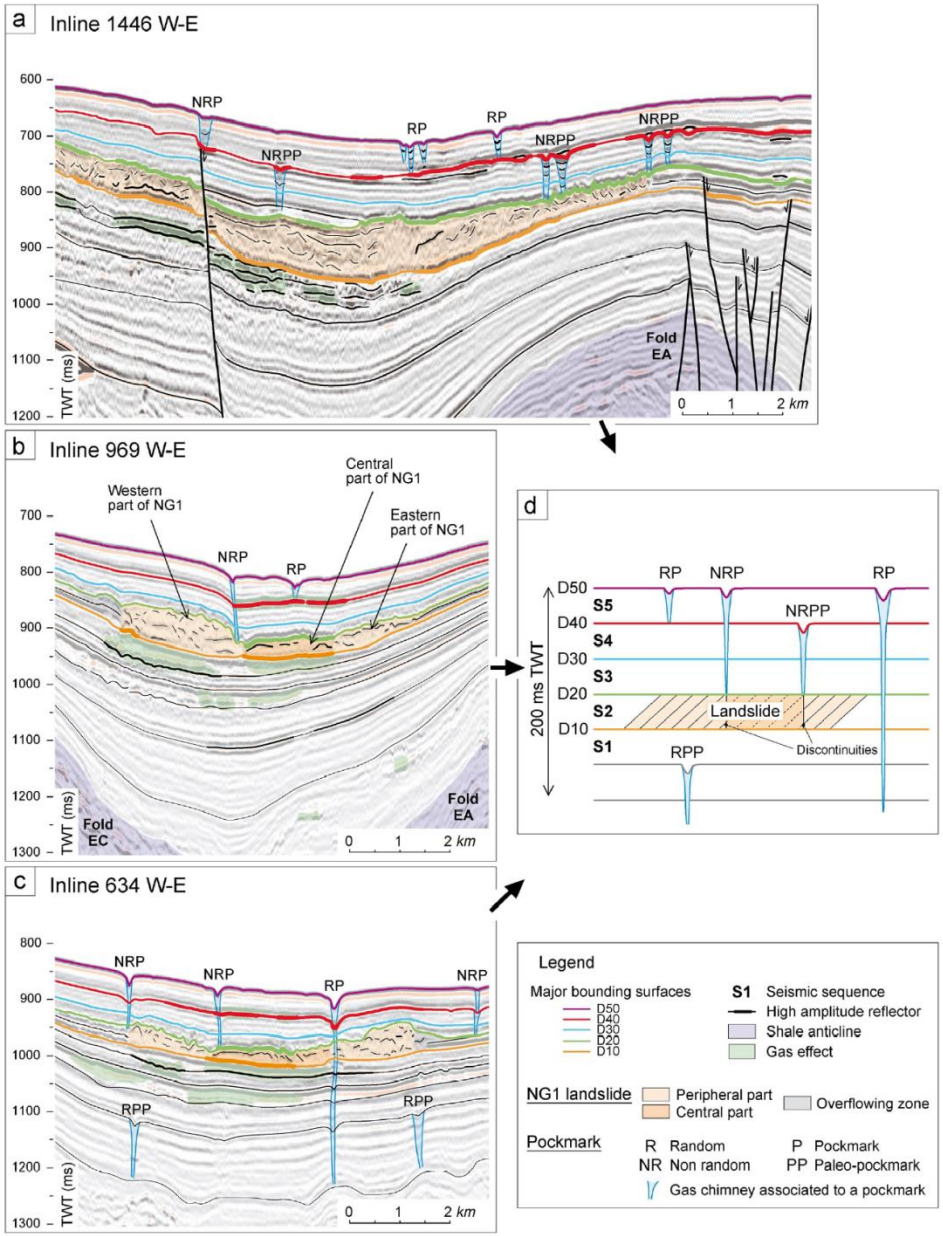

Fig. 6. (a) Seismic transversal inline 1446 oriented W–E, from reprocessed exploration 3D seismic data, with its seismic interpretation showing (1) non-random pockmarks connected with NG1 landslide ending up in D40 reflector, and (2) random pockmarks rooted in the D40 reflector. (b) Seismic transversal inline 969 oriented W–E, from reprocessed exploration 3D seismic data, with its seismic interpretation showing (1) non-random pockmarks rooted in NG1 landslide internal discontinuities, and (2) pockmarks rooted in the D40 reflector. (c) Seismic transversal inline 634 oriented W–E, from reprocessed exploration 3D seismic data, with its seismic interpretation showing (1) non-random pockmarks rooted in NG1 landslide internal discontinuities, (2) random paleo-pockmarks, and (3) random pockmarks deeply rooted. (d) Summary of organization of the stratigraphic pattern and location of all types of pockmarks observed in the study area. See text for details.

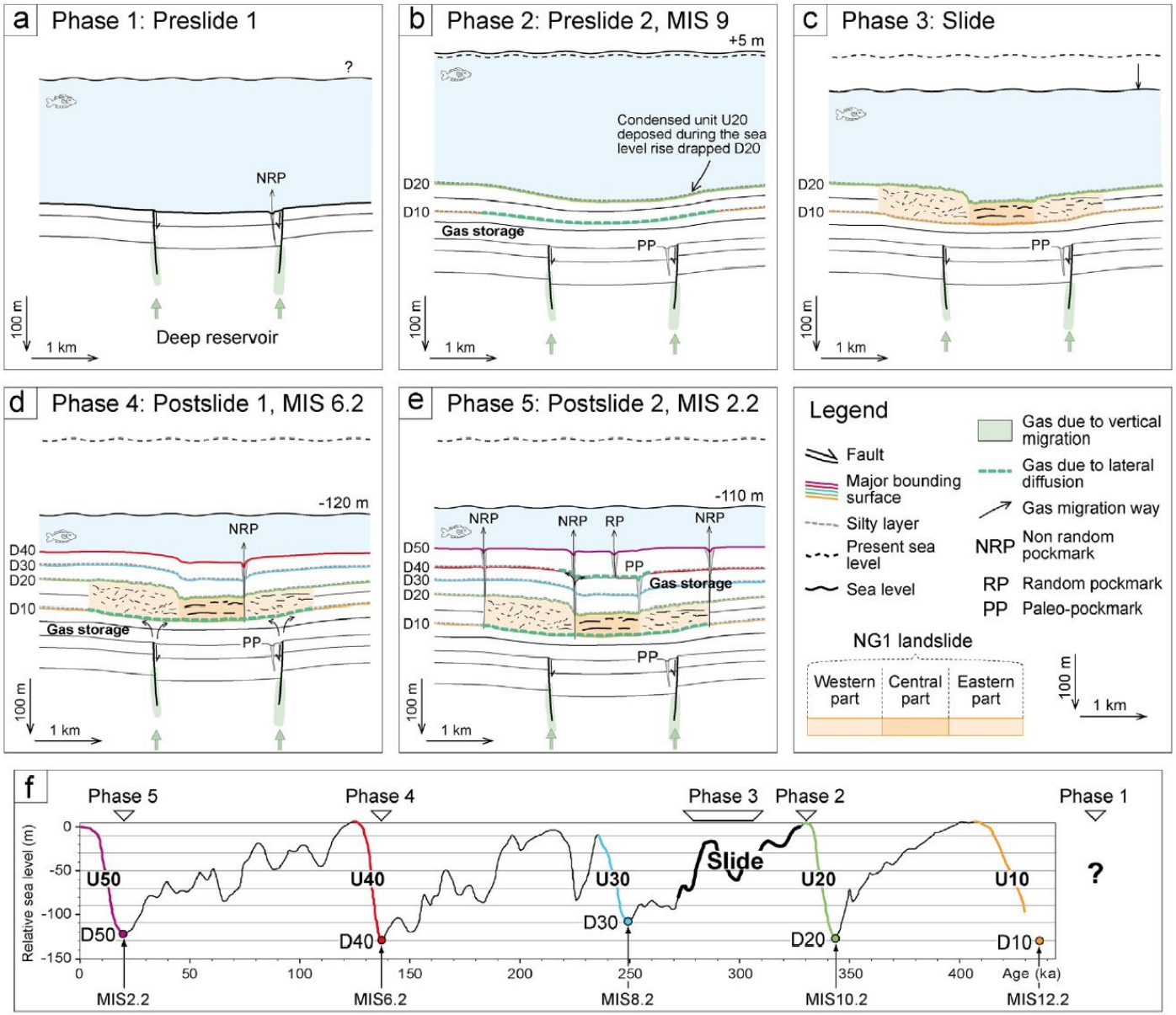

Fig. 9. Conceptual model (Idealized scenario) of development of pockmark field controlled by fluid seepages throughout a landslide. The scenario, valid for the observations made in this paper, is composed of 5 phases (a–e) detailed in the discussion. (f) Sea-level change curve (Waelbroeck et al., 2002) indicates the timing of phases 1–5 of pockmarks and landslide formation.

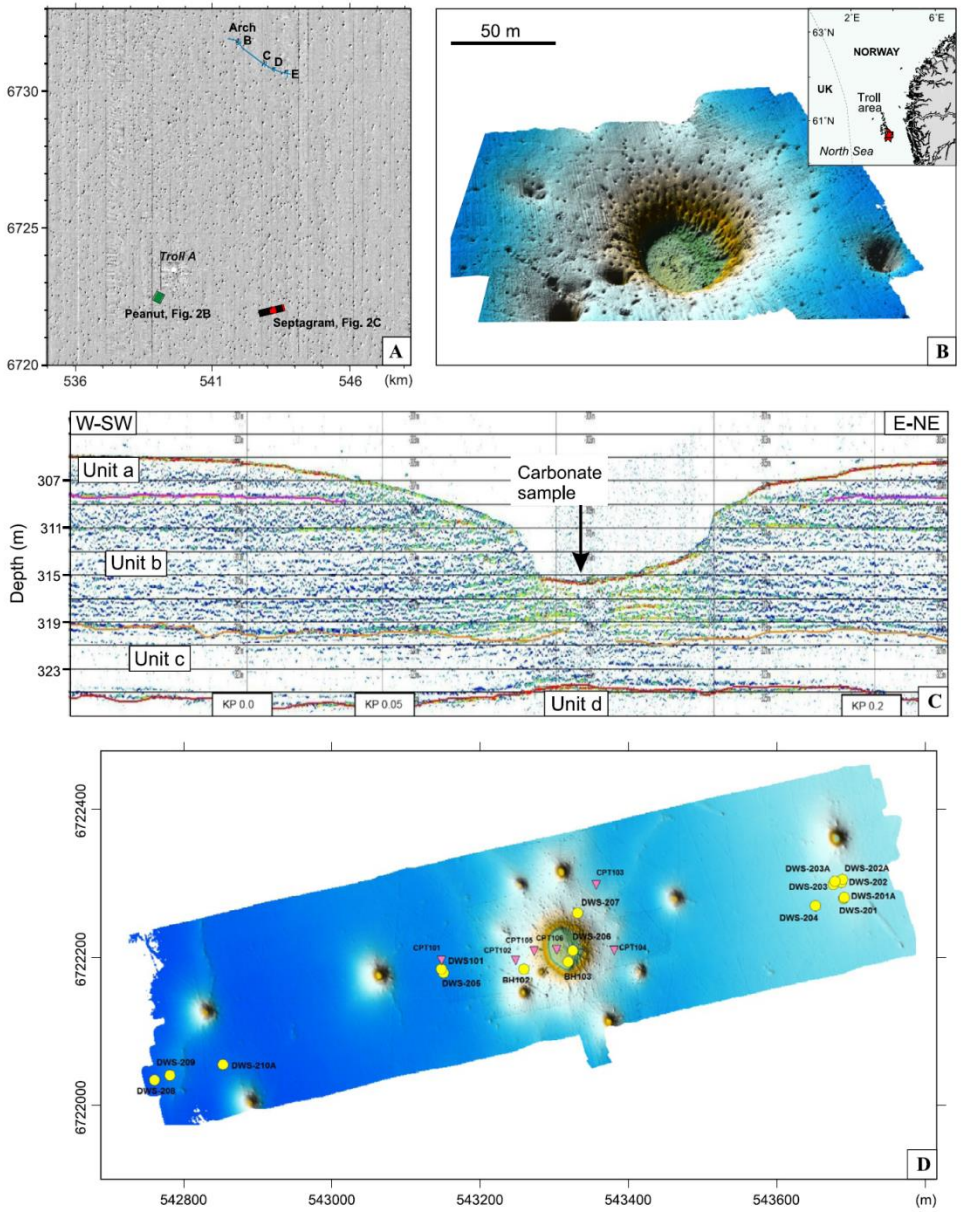

Fig. 1. **(A)** Fragment of Troll field multibeam coverage where more than 7000 pockmarks (2.5 m gridding resolution) have been mapped. Indicated are the Troll A platform and the pockmark areas more intensively studied. Inset map offshore Norway. UTM Zone 31, WGS84 datum. **(B)** Example of high-resolution bathymetry (0.2 m resolution) of the Septagram pockmarks showing a 15 m deep circular depression with a flat interior. For location refer to Fig. 1A. **(C)** Example of ROV sub-bottom profile through the Septagram pockmark. Indicated are the four imaged units (a–d). For size refer to Fig. 1B. The pockmarks typically cross-cut the reflections of Unit b. See text for geochronology of these units. **(D)** Multibeam line across the Septagram region and locations of the cores available that were collected in the area for radiocarbon dating and CPT (pink triangles). The scales for the maps in the manuscript are in metres or kilometres, UTM Zone 31, WGS84 datum. (For interpretation of the references to colour in this figure legend, the reader is referred to the web version of this article.)

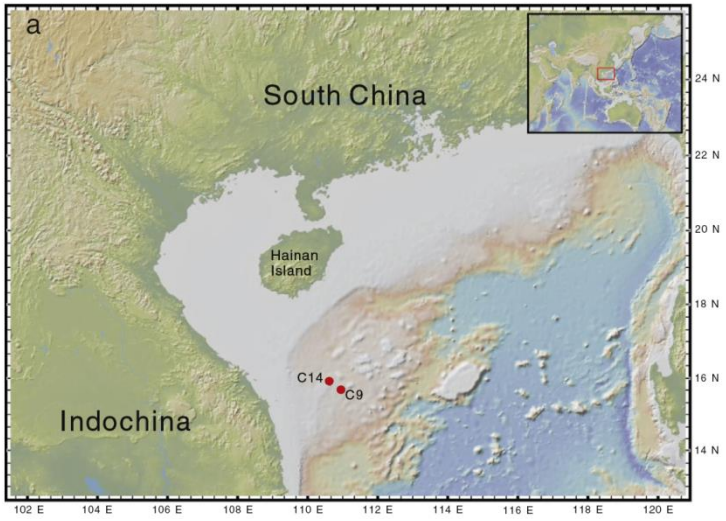

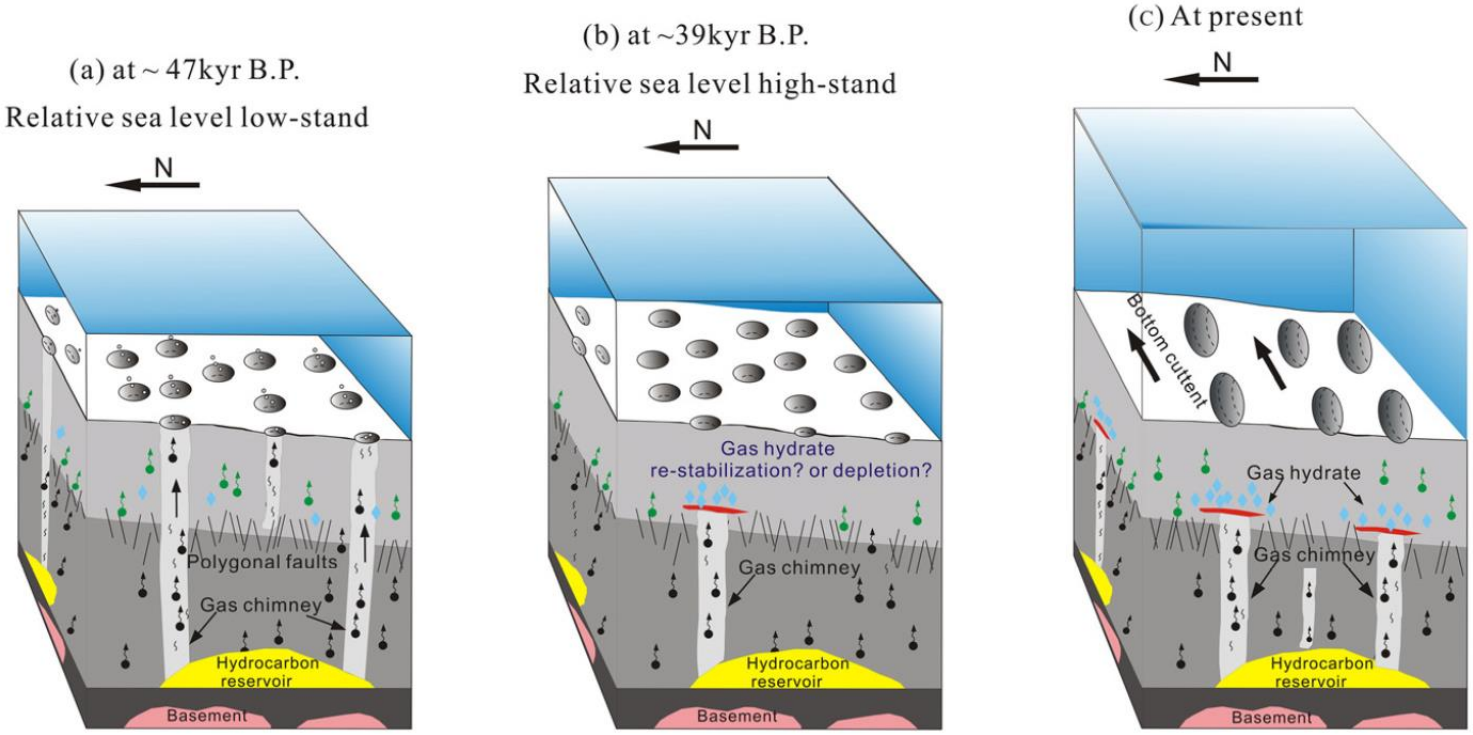

Fig. 7. Proposed schematic representation of the evolutionary history of fluid seepage in the study area. (a) At ca. 47 kyr B. P. fluid seepage occurred due to gas hydrate dissociation during relative sea level low-stand. This age based on authigenic carbonate dating is assumed to be the timing of the last fluid seepage event in the pockmark field. (b) At ca. 39 kyr B. P., fluid seepage ceased owing to either gas hydrate re-stabilization during relative sea level high-stand or the total depletion of gas hydrate reservoir. (c) Recharging of gas hydrate reservoir within the gas hydrate stability zone in the pockmark field during present-day sea level high-stand. Pockmarks have since evolved into mega-pockmarks after being reshaped by bottom currents.

Gas hydrate distributions in sediments of pockmarks from the Nigerian margin – Results and interpretation from shallow drilling

Jiangong Wei [a, *], Thomas Pape [a], Nabil Sultan [b], Jean-Louis Colliat [c], Tobias Himmler [a, b], Livio Ruffine [b], Alexis de Prunelé [b], Bernard Dennielou [b], Sebastien Garziglia [b], Tania Marsset [b], Carl A. Peters [a, e], Abdulkarim Rabiu [d], Gerhard Bohrmann [a]

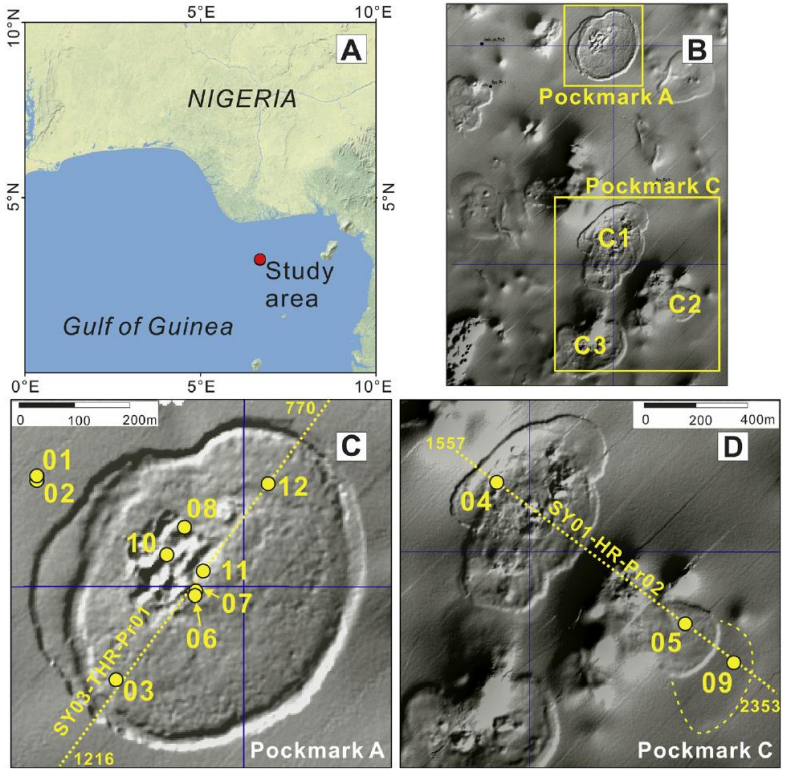

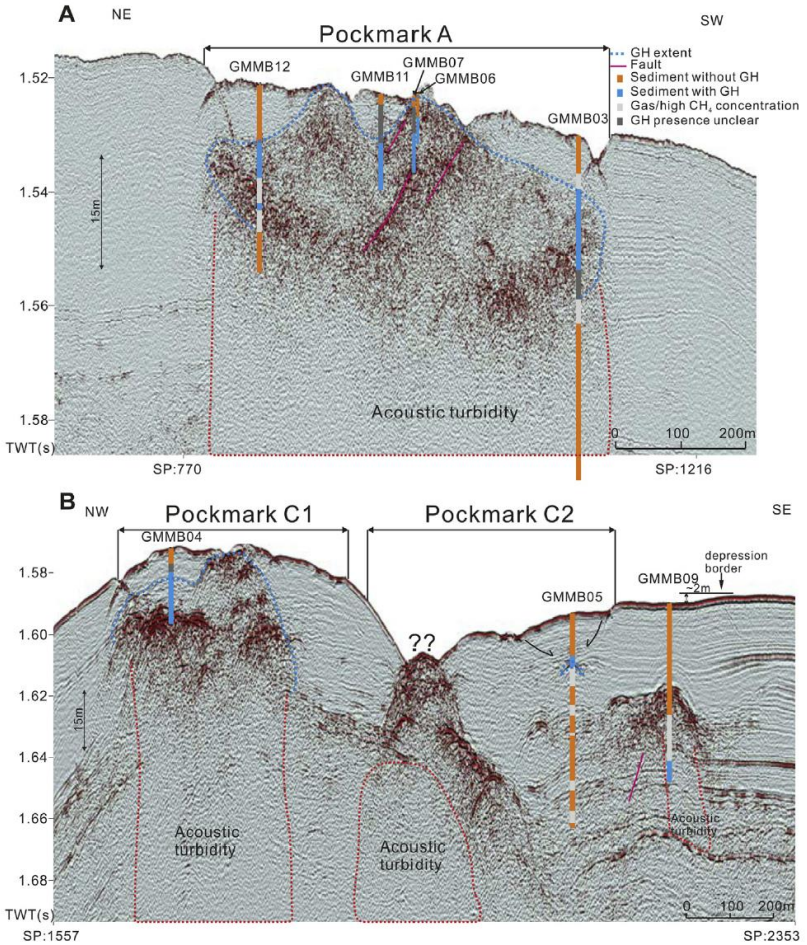

Figure 7. SYSIF seismic profiles SY03-THR-Pr01 crossing pockmark A and SY01-THR-Pr02 covering pockmark cluster C. Locations and orientations are shown in Figure 1. Interpretations from MeBo cores are projected on the seismic profiles. High-amplitude reflectors are widespread in the seismic profile.

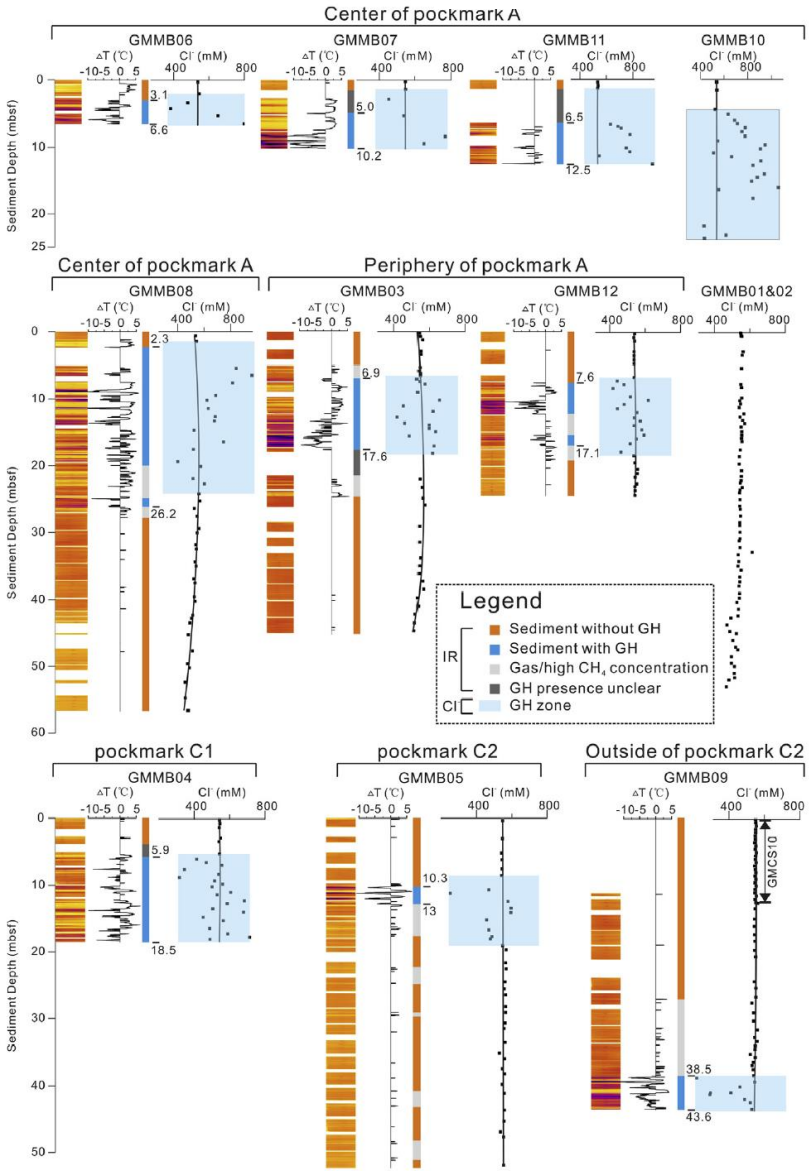

Figure 3. IR temperatures and pore water chloride concentration profiles of MeBo cores. Four data sets are shown for most drill sites: IR image colors, IR temperature profiles, interpreted gas hydrate distributions, and chloride profiles. The color bar of the IR images is consistent with Figure 2 and white intervals indicate gaps. Temperature profiles show the differences between the measured temperature and background temperatures of core liners, expressed as ΔT. Positive ΔT values correlate with voids in the cores and negative ΔT values represent decomposing gas hydrates. The approximate down-core gas hydrate presence interpreted from IR images is indicated by colored bars and by indications for depth below seafloor (mbsf). Depths of gas hydrate-bearing intervals as inferred from chloride anomalies are highlighted in blue shading. Note that the chloride data of the upper 12.7 mbsf at station GMMB09 were derived from a piston core (GMCS10) taken at the same position. (For interpretation of the references to color in this figure legend, the reader is referred to the web version of this article.)

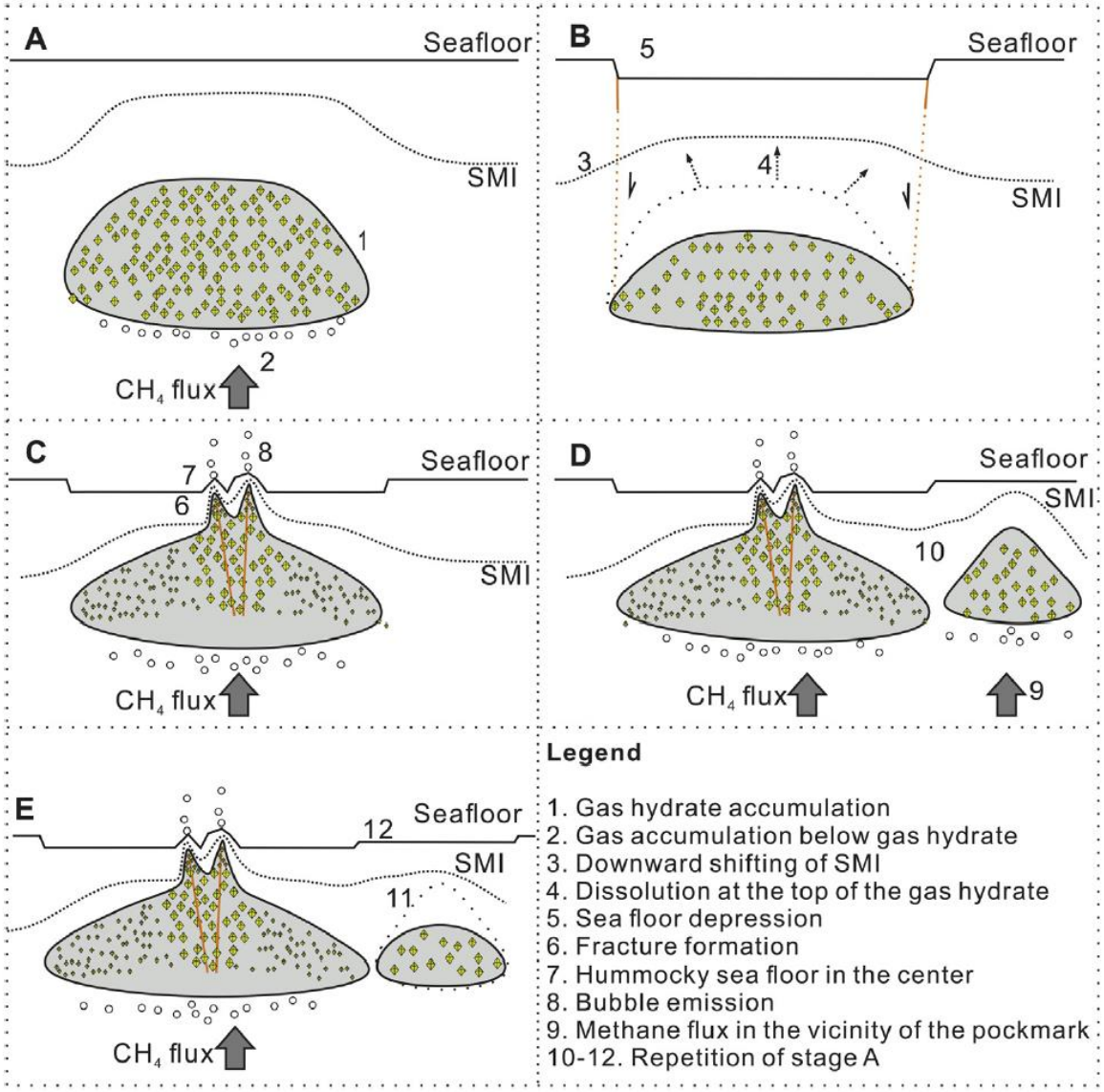

Figure 8. Schematic representations of the pockmark formation controlled by fluid flow and gas hydrate precipitation during different evolutionary stages (A–E).

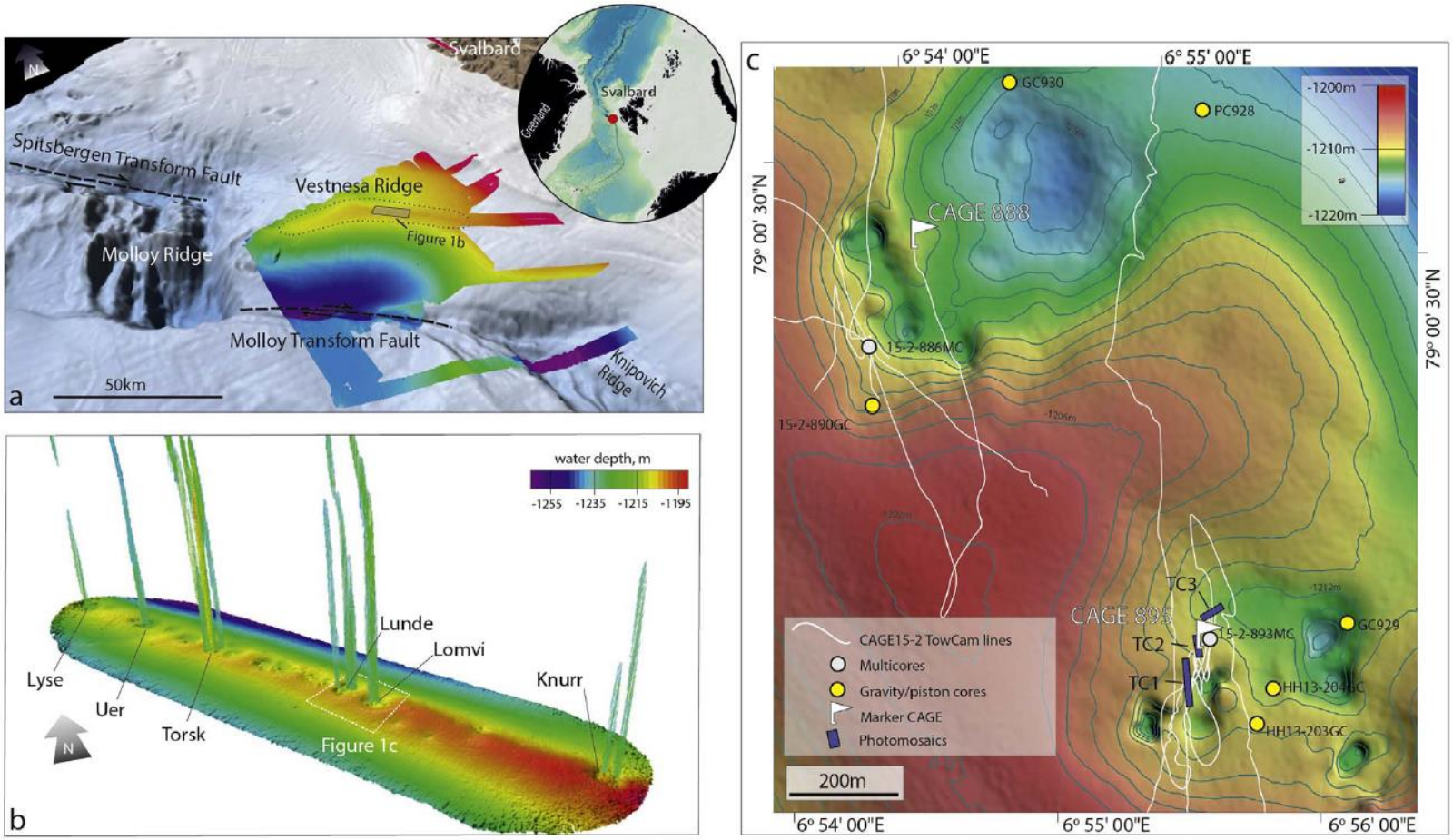

Fig. 1. a) Location map showing Vestnesa Ridge in the Fram Strait. b) Names of active pockmarks along the eastern crest of Vestnesa Ridge; c) regional multibeam bathymetric map showing sampling locations. Location of sediment cores used in this paper (see Table 1), ship track lines of the six bottom photography tows that collected over 5000 images, and the photomosaics TC1–3 are indicated. To be noted the location of marker CAGE888 and CAGE895.

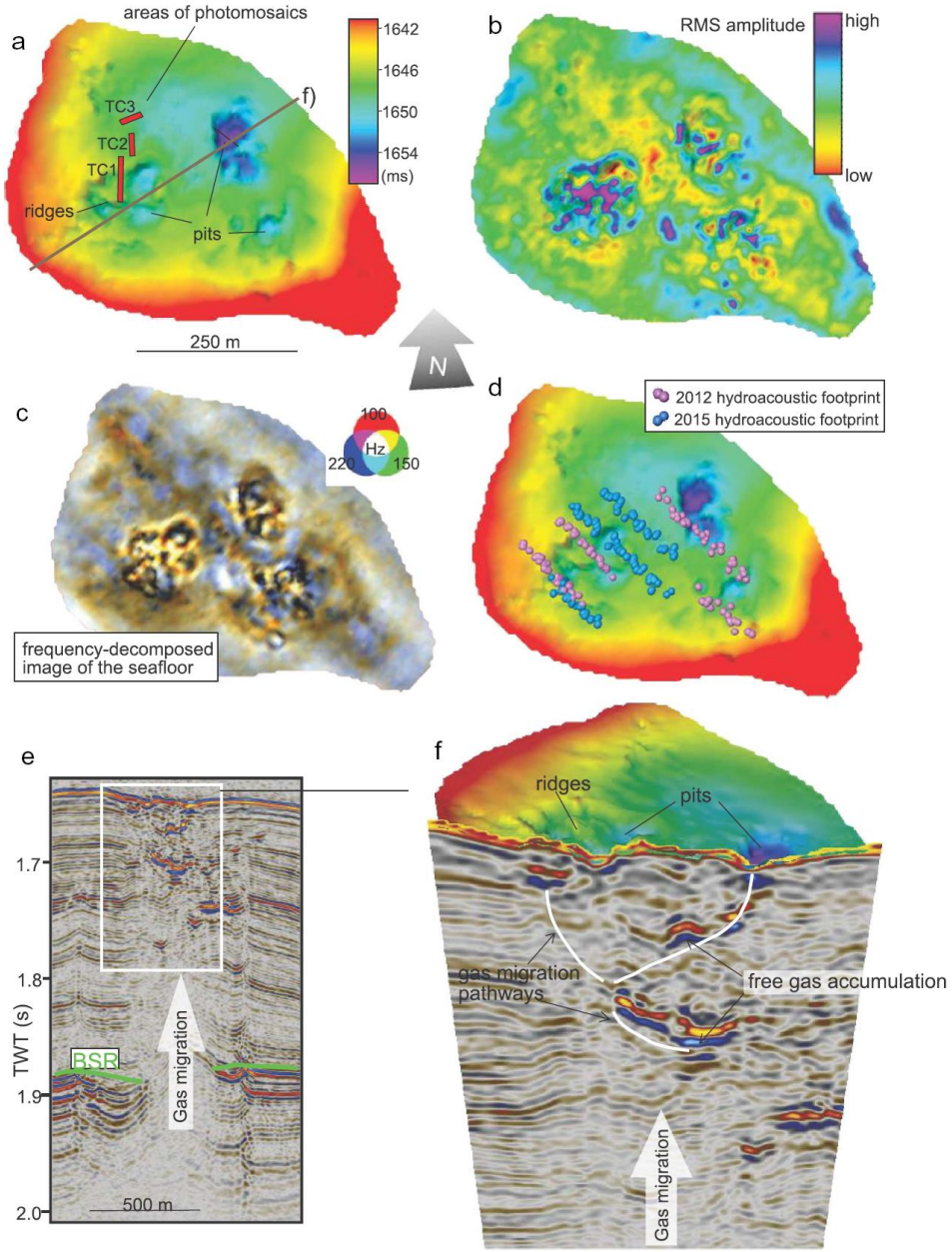

Fig. 2. a) Bathymetry of Lomvi pockmark. The photomosaics TC1–3 and the subsurface seismic shown in e and f of this figure are indicated. b) RMS (root mean square) amplitude of Lomvi. The purple color shows high amplitude most likely related to the presence of free gas within the sediment. c) Frequency decomposed image of the seafloor where areas that appear whitish in color show good response in all three frequencies indicating free gas, gas hydrate or carbonates, whereas areas that show darker color have poor response in all frequencies. d) pink and light blue dots represent the centre of the hydroacoustic footprints (radius of 73 m) of gas bubbles. e) Seismic profile showing the chimney structure; the white box is shown in f) and outlines high amplitude anomalies in the gas chimney beneath Lomvi that stack and align vertically, cutting across disrupted strata and terminating into the pits at the seafloor. White lines indicate migration pathways.

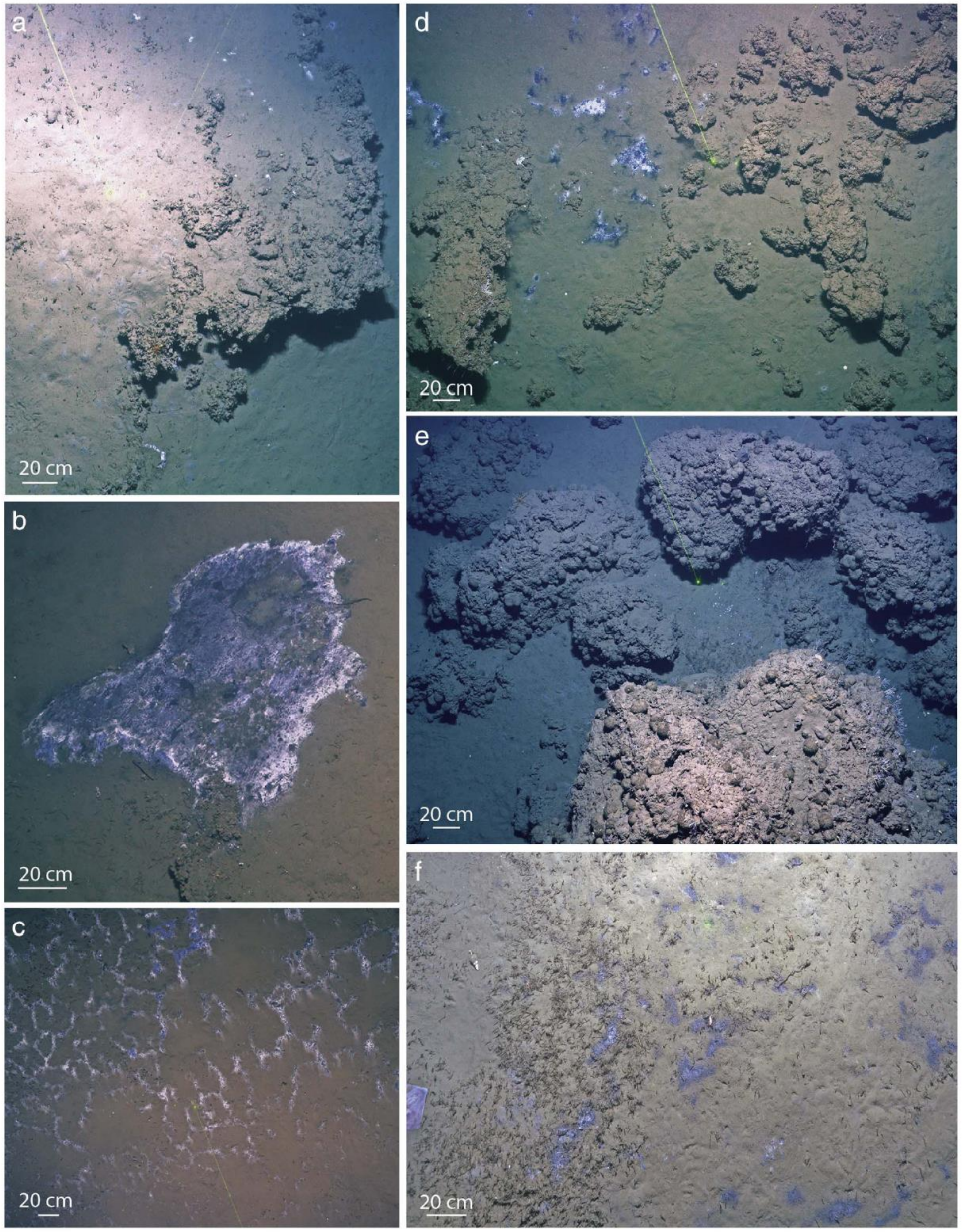

Fig. 4. a) Carbonate crust, ca 5–10 cm thick. Sediment underneath the crust has been scoured. b) Large patch of white bacterial mats; throughout the image highlighted against the iron sulfide bearing black sediment. Two fish appear to feed on bacterial mats. c) Bacterial mats exhibit a network structure. d) Sparse small carbonate blocks associated with patches of bacteria. Benthic animal tracks are obvious in the image. e) Massive carbonate blocks with ca 2 m of elevation provide a hard substrate for epifaunal invertebrates (e.g., erect bryozoans and spherical sponges) and for mobile fauna. f) Soft sediment, mud bottom with dense bushes of siboglinid tubeworms and patches of bacterial mats.
Green laser dots spaced 20 cm apart (these are present in all images and provide the ability to scale features in all images; when not present the scale is indicated).

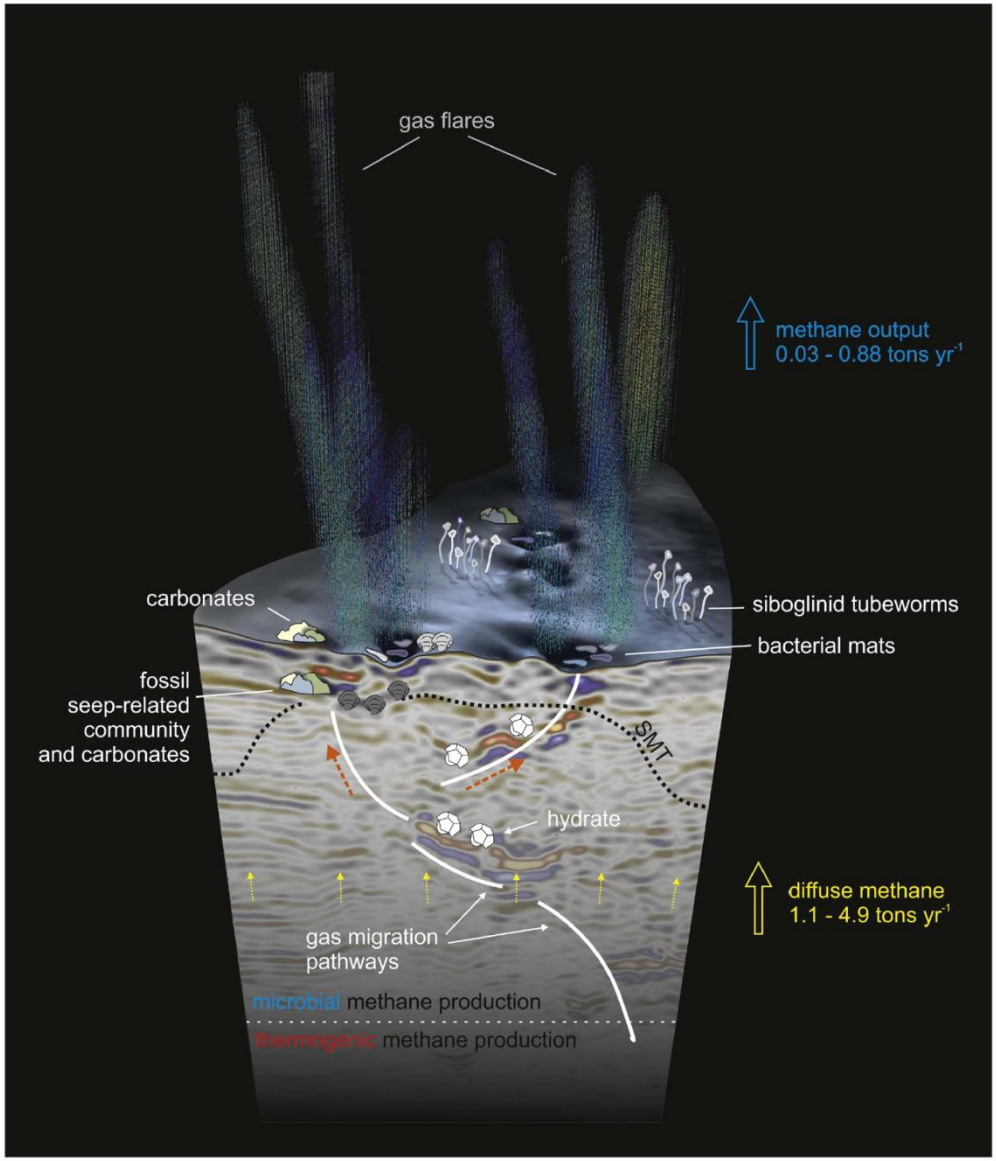

Fig. 9. Cartoon showing the main characteristics and processes occurring in Vestnesa pockmarks. The seismic profile (from Fig. 2f) shows the chimney underneath the Lomvi pockmark. In the top half of the chimney enhanced reflections appear to cut across lithological boundaries and are slightly inclined upwards towards the seafloor where they terminate in the pits. The enhanced reflection results from a strong impedance contrast due to the presence of free gas, gas hydrates and/or carbonates. The white lines indicate migration pathways. The finding of fossil seep-related community and carbonate nodules (Ambrose et al., 2015) might explain some of those reflections. The diffuse (yellow arrows) and focused (orange arrows) fluid flows are indicated, the numbers are from Table 3, and the size of the fluxes are explained in the text, including relevant references. SMT = sulphate-methane transition zone. The thermogenic production of methane occurs in deep sediment and feeds the gas hydrates while microbial methane production occurs in the entire sedimentary column. (The cartoon is not on scale).

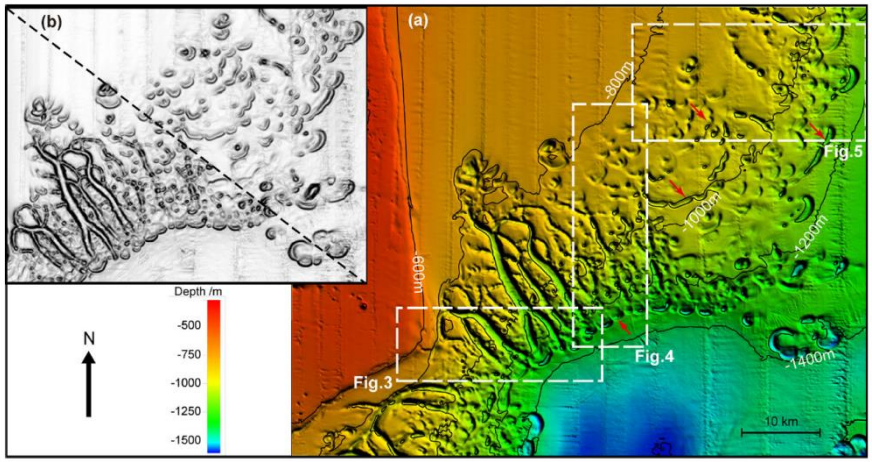

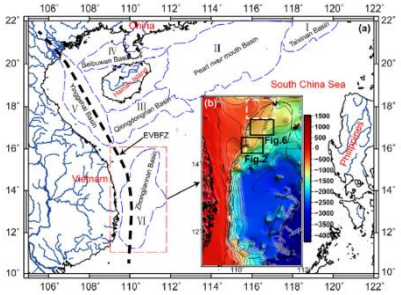

Fig. 2. Southernmost study area in the ZB-see Fig. 1 for location. (a) Crescent pockmarks, isolated or forming pockmark strings (red arrows) as well as a few submarine gullies are identified on the multibeam bathymetric map of the study area (see location in Fig. 1). Detailed bathymetry and combined seismic lines (dashed rectangles) are shown in Figs. 3–5 respectively. (b) Mainly located in the northeast part of this study area and parallel to the isobaths, crescent pockmarks and pockmark strings can be easily recognized on the slope map of the study area. (For interpretation of the references to color in this figure legend, the reader is referred to the web version of this article.)

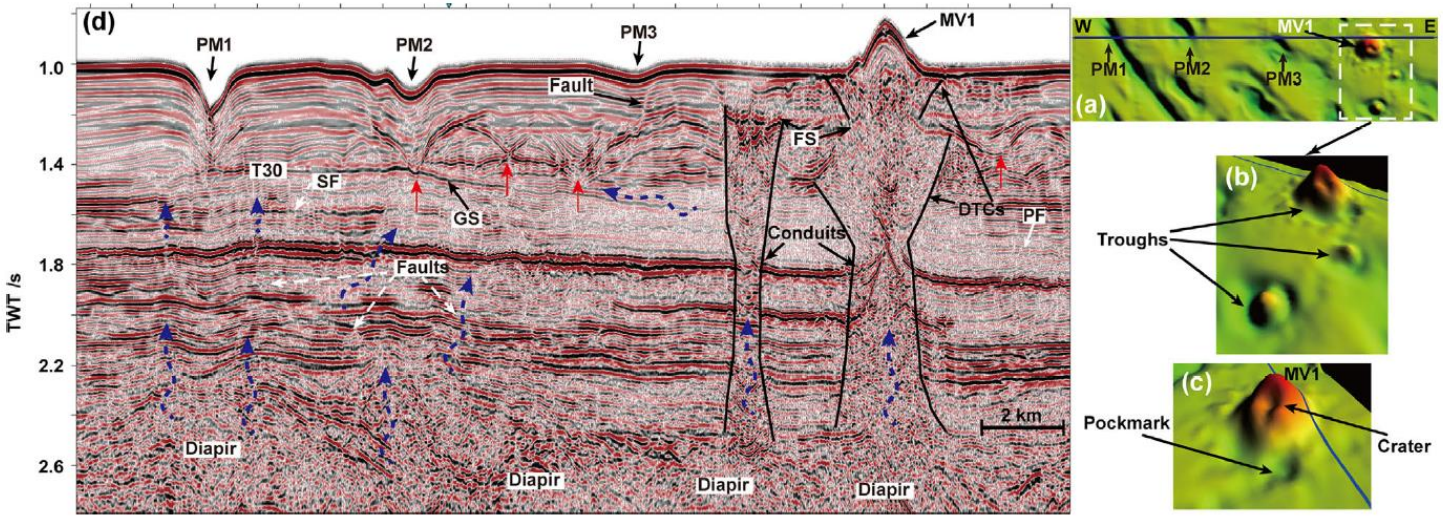

Fig. 7. Northern study area (see location in Figs. 1 and 6). (a) Elongated pockmark (PM1), elliptical pockmark (PM2), irregular pockmark (PM3) and three isolated mud volcanoes (MV) are identified on the detailed bathymetry and seismic data (see location in Fig. 2). The study area outlined in the dashed white rectangle is expanded in (b) and the detailed morphology of MV1 is expanded in (c). The associated troughs, pockmark and crater can be easily recognized. (d) Multichannel seismic line. Fluids escaping from the deep diapirs flow along the conduits, consisting of vertical or sub-vertical faults, small fractures (SF) and sediments with high porosity and permeability, accumulate in the shallow sediments, cause sediment remobilization and produce seepage structures such as pockmarks or mud volcanoes. The model proposed to interpret the evolution of mud volcanoes in the northern ZB and particularly the first stage (FS) was based largely in the seismic and bathymetric data shown in Fig. 7d and in Fig. 8b and d. PF=polygonal faults. DTCs=downward tapering cones. (For interpretation of the references to color in this figure, the reader is referred to the web version of this article.)

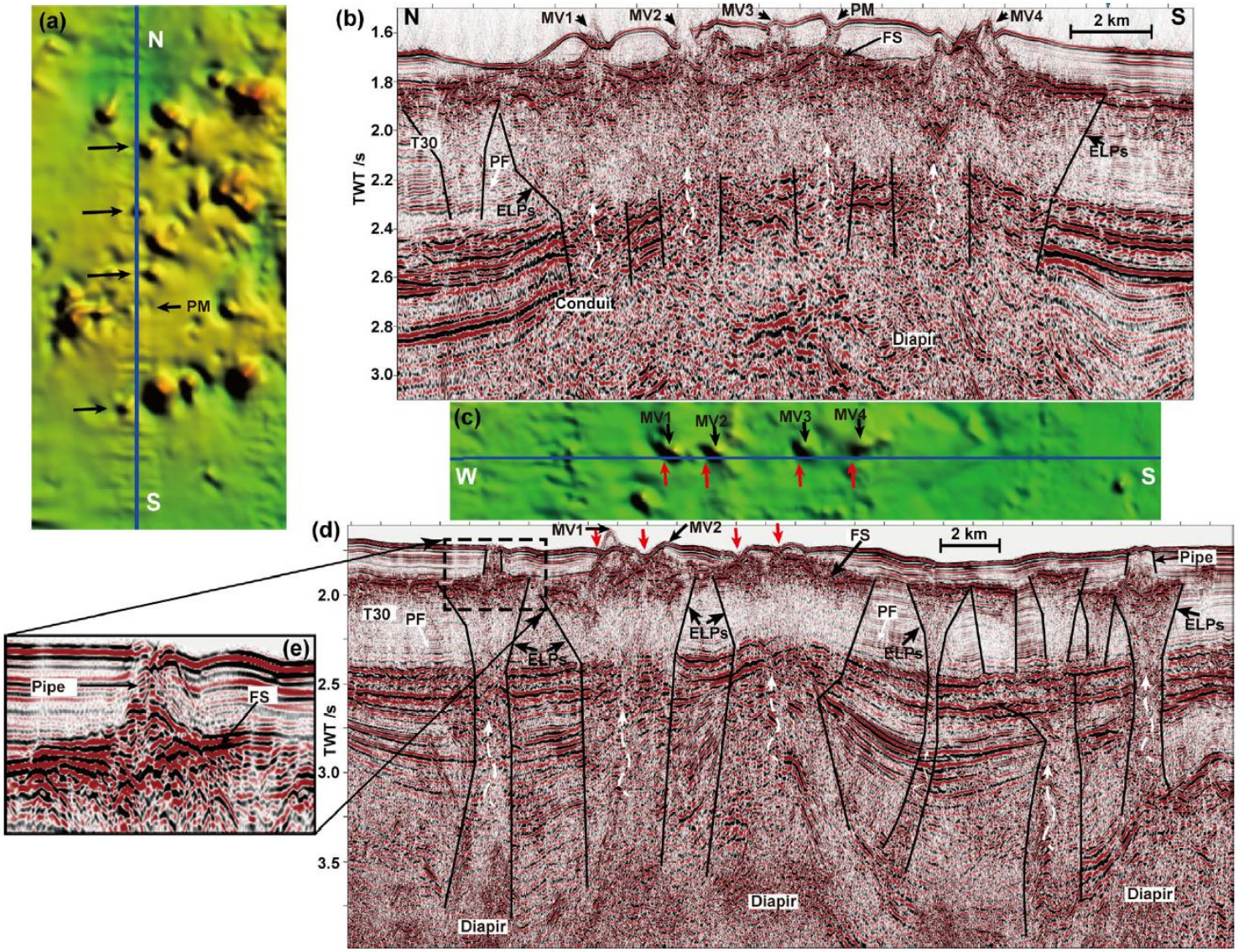

Fig. 8. Northern study area (see location in Figs. 1 and 6). Detailed bathymetry (a, c) and corresponding seismic data (b, d) used to characterize the structure of the MVG2 (see location in Fig. 2). The first stage (FS) is easy to recognize (see Section 5 in the text). (b) Four mud volcanoes (MV) and one pockmark (PM) with a gas pipe acting as a fluid pathway are developed in the second stage. (d) Troughs (red arrows) are associated with faults and the enhanced reflections indicate fluid pathways around the mud volcanoes. (e) Expanded image outlined by the dashed black rectangle in (d) show first stage complex sediment structure and a pipe feeding a pockmark above in second stage. In summary, two types of conduits are recognized and these are analyzed in Section 5 and proposed model. PF=polygonal faults. ELPs=emanative leakage passages. (For interpretation of the references to color in this figure legend, the reader is referred to the web version of this article.)

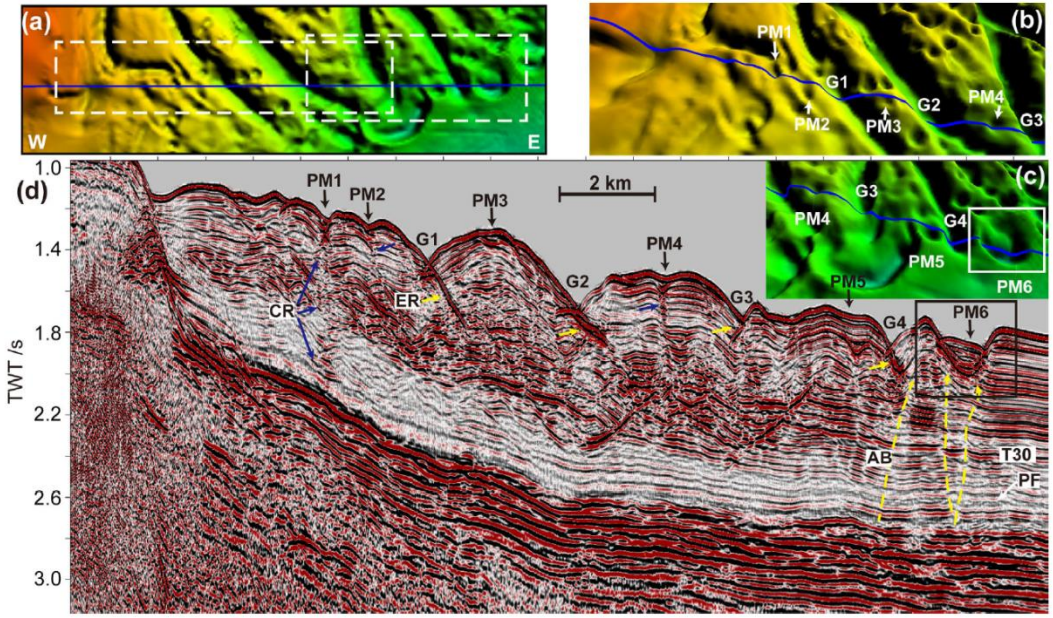

Fig. 3. Southern study area (see location in Figs. 1 and 2). Pockmarks (PM) and gullies (G) are clearly identified and studied on the detailed 3D topography (b) and (c), outlined by dashed rectangles in (a). (d) The location of the seismic line is indicated by the blue line in (a). Pockmarks (PM) are associated with chaotic reflections (CR, blue arrows), acoustic blanking (AB, yellow dashed arrows) and vertical high amplitude reflections within the gas chimneys; the latter could represent carbonate formation. Inclined faults with enhanced reflections (ER, yellow arrows) are observed just beneath the gullies and probably acted as the main fluid feeding pathways. Detailed analysis of the crescent pockmark (PM6) outlined by the black rectangle will be shown in Fig. 9. PF = polygonal faults. (For interpretation of the references to color in this figure legend, the reader is referred to the web version of this article.)

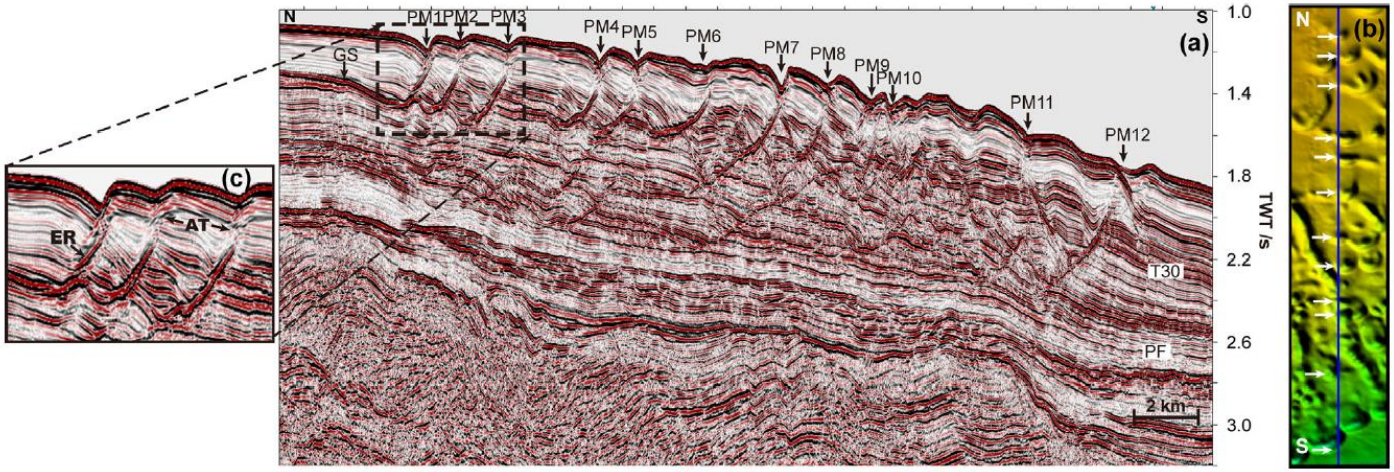

Fig. 4. Southern study area (see location in Figs. 1 and 2). All the pockmarks (PM) with various morphologies (black arrows) seen on the detailed 3D topography (a) are associated with inclined faults with characteristics of listric faults and curved fault plane, with acoustic turbidity (AT) near the top and enhanced reflections (ER) in the base. (c) Magnified image of the seismic data (a) indicated by dashed rectangle, shows detailed structure of the inclined faults. Enhanced reflections within the inclined faults show a strong connection with the gas-charged sediments (GS). PF = polygonal faults.

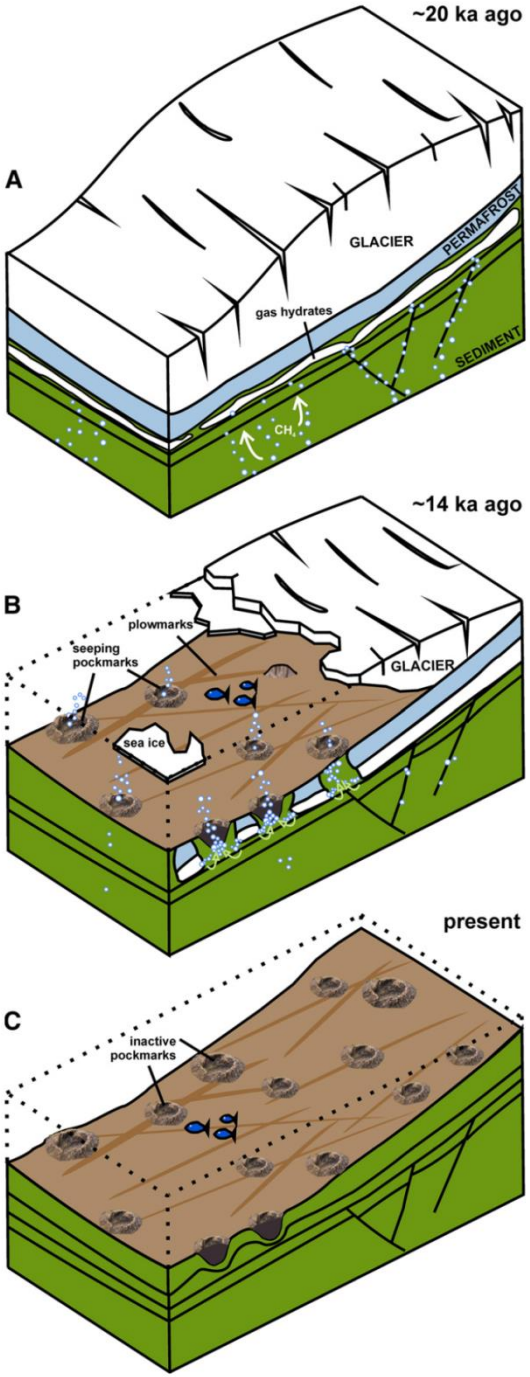

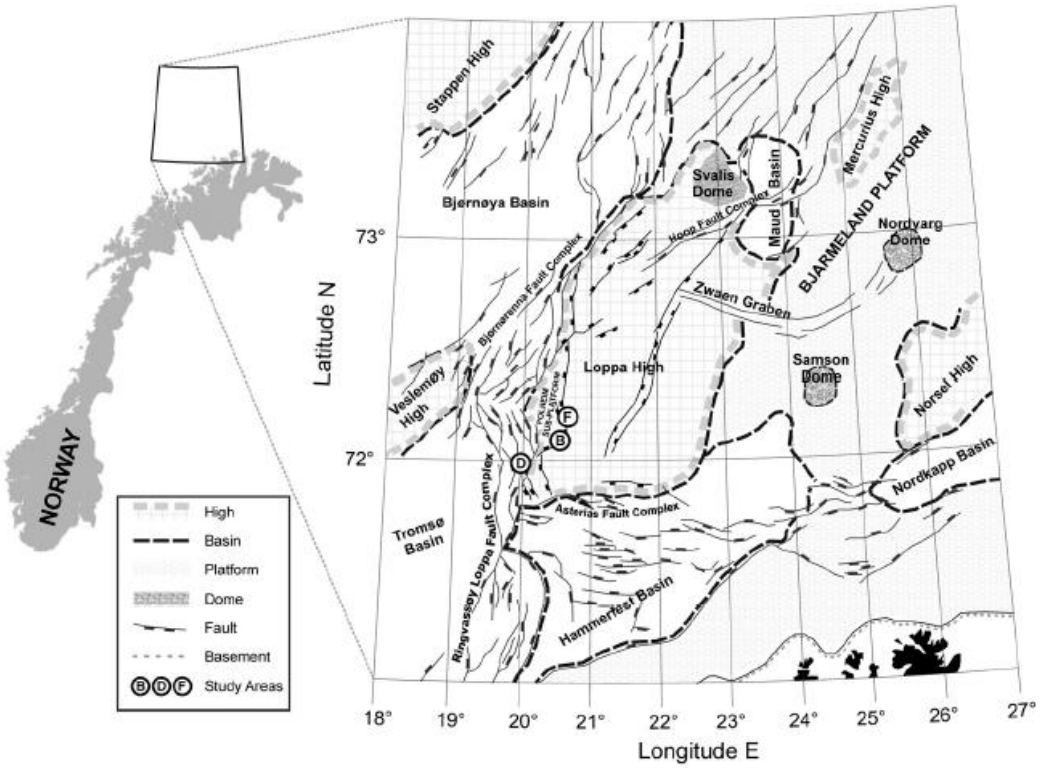

Fig. 6. (A) During LGM a grounded ice sheet covered the area. Upwards migrating methane accumulated under the ice and formed gas hydrates. (B) During the glacial retreat the gas hydrates decomposed, releasing large volumes of gas, resulting in the formation of pockmarks. (C) Present day situation in the study area. No detectable seeping activity but pockmark structures still preserved.

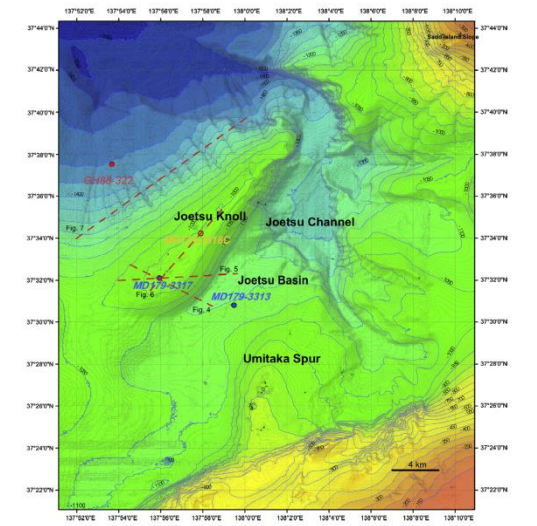

Fig. 2. Submarine topography of the Joetsu Knoll and adjacent area (Hiromatsu et al., 2011) with locality of core sites in this paper. The 3.5 kHz SBP lines are shown as dotted lines. Red broken lines show profile segments in the following figures. Contours are in meters.

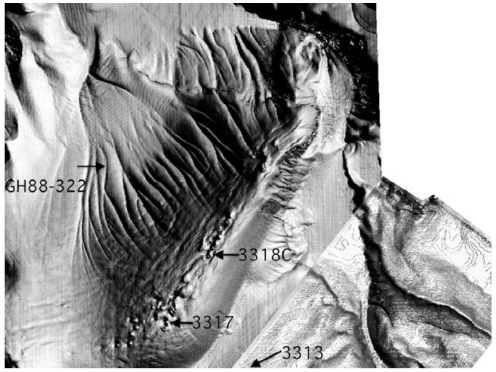

Fig. 3. Shaded sea surface image from 3D seismic data showing pockmarks/mounds on the axis of the Joetsu Knoll and submarine canyons on the western flank of the Joetsu Knoll. Some canyons are connected with mounds. Arrows indicate locations of the cores presented in Fig. 2.

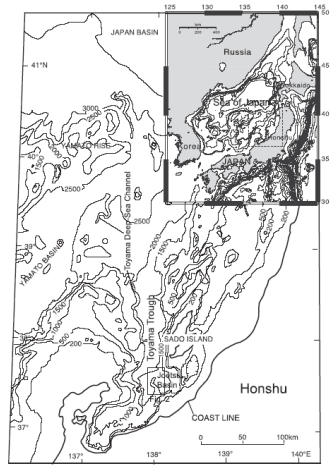

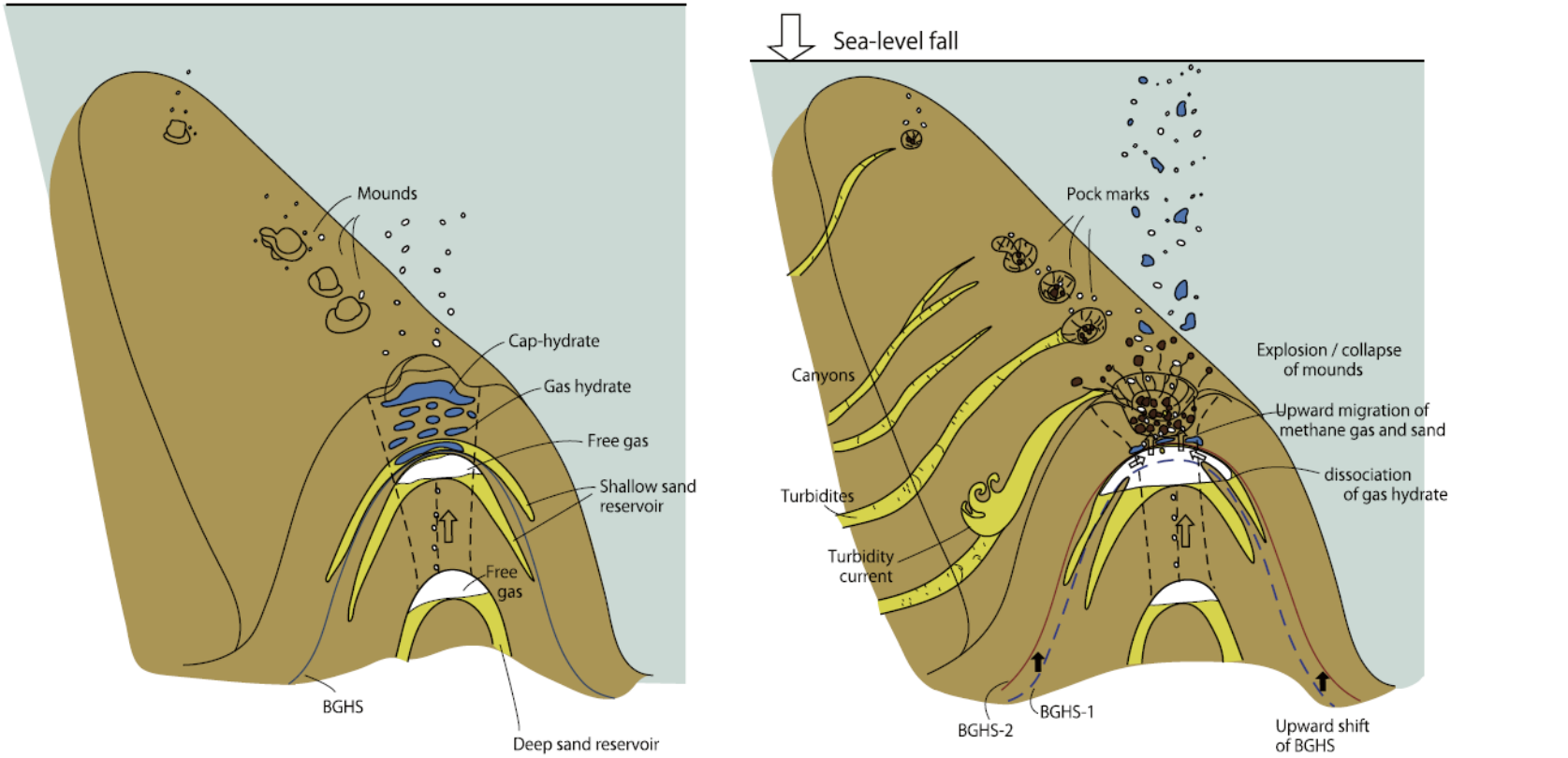

Fig. 13. Conceptual model showing the formation of pockmarks and submarine canyons on the Joetsu Knoll.

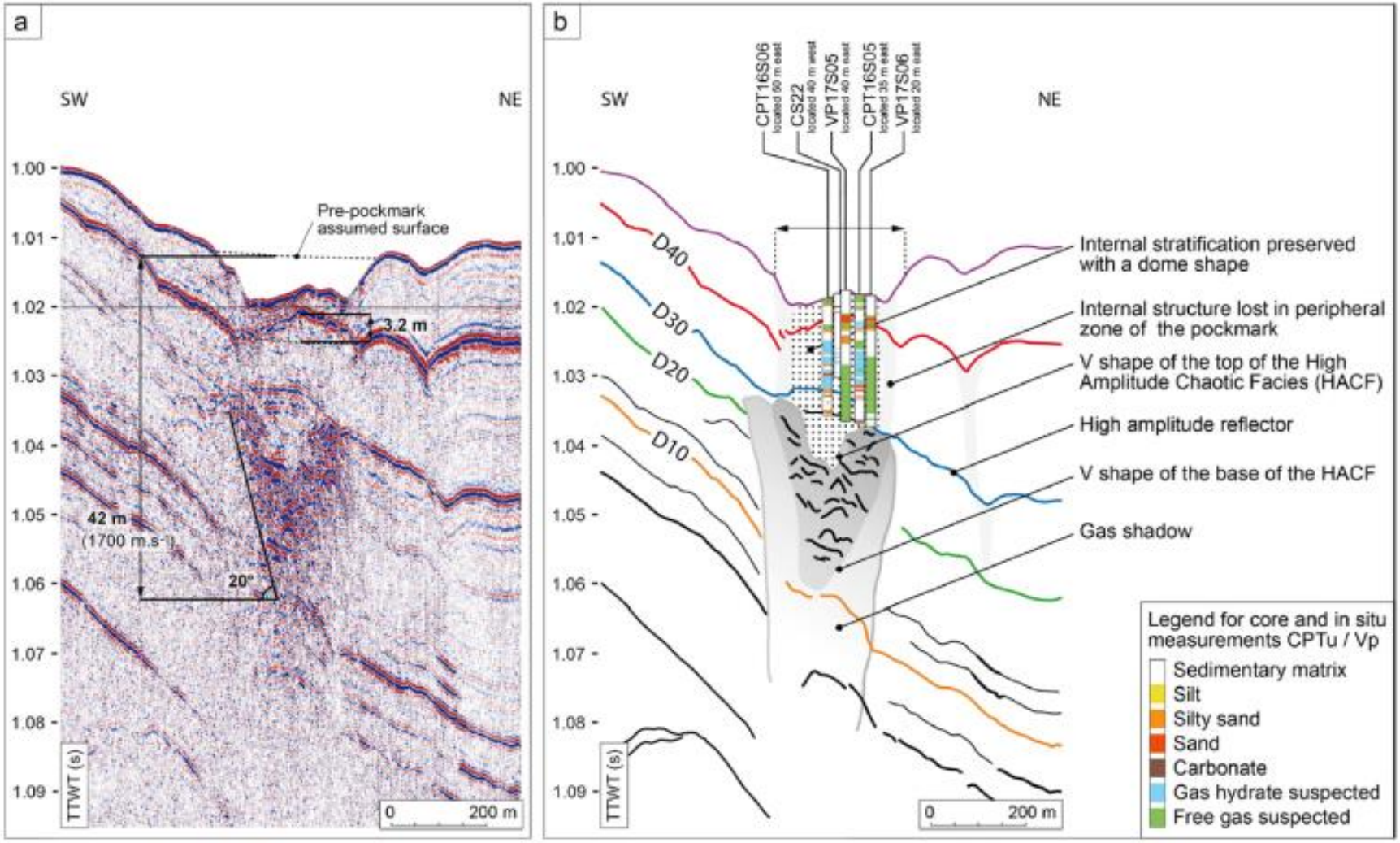

Fig. 3. 2D high resolution seismic profile (Sysif profile SY11-Pr03 – for location see Fig. 2) with its stratigraphic interpretation showing the studied pockmark internal structure with the location and interpretation of in situ measurements and sedimentary cores. CPTu: Piezocone penetration testing and Vp: Velocity of the primary wave.

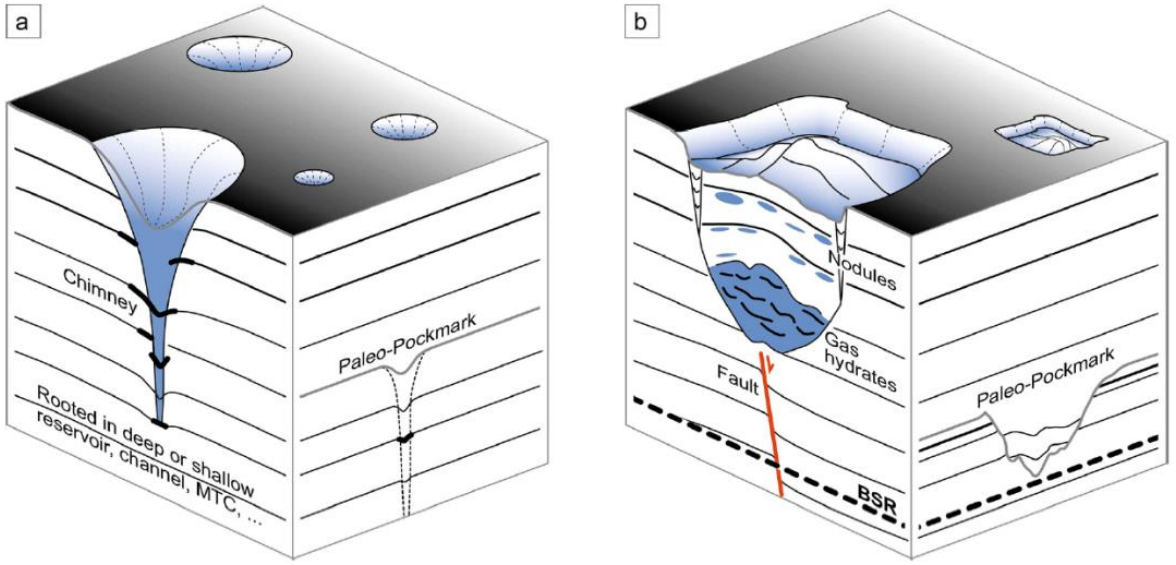

Fig. 2. Geometrical characteristics of the two types of pockmarks described in the literature. a: Type-1 pockmarks describe circular depressions associated to a gas chimney and are commonly observed on continental margins since 1970. Figure modified from Cathles et al. (2010). b: Type-2 pockmarks correspond to irregular and distorted depression associated in depth to the presence of gas hydrates.

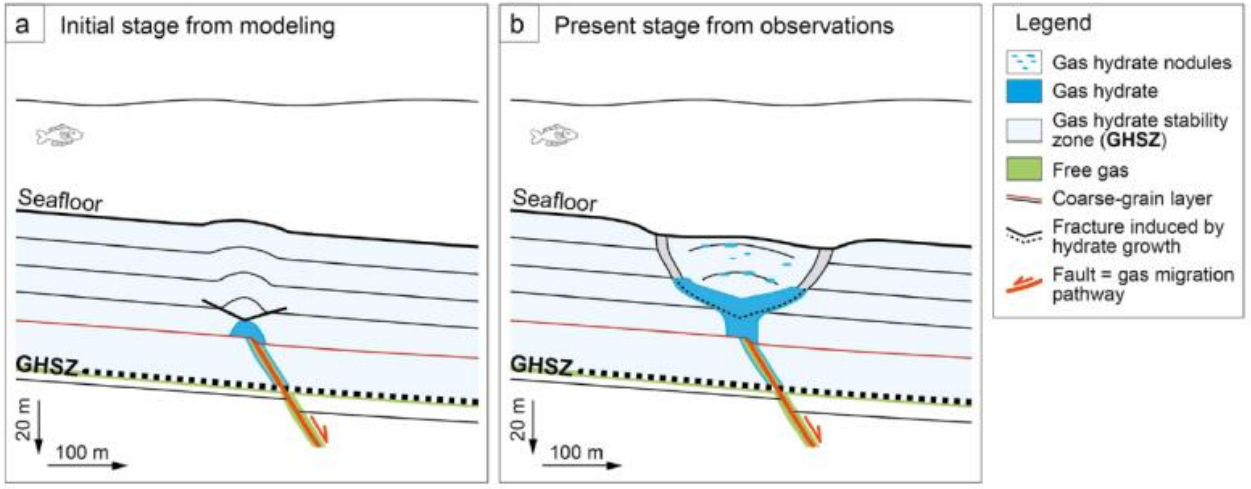

Fig. 10. Conceptual model (Idealized scenario) of development of Type-2 pockmark controlled by fluid seepages throughout a fault in the GHSZ. The scenario is composed of 2 phases (a, b) detailed in the discussion.

Черное море.
Наумова, 2019,
Лукойл

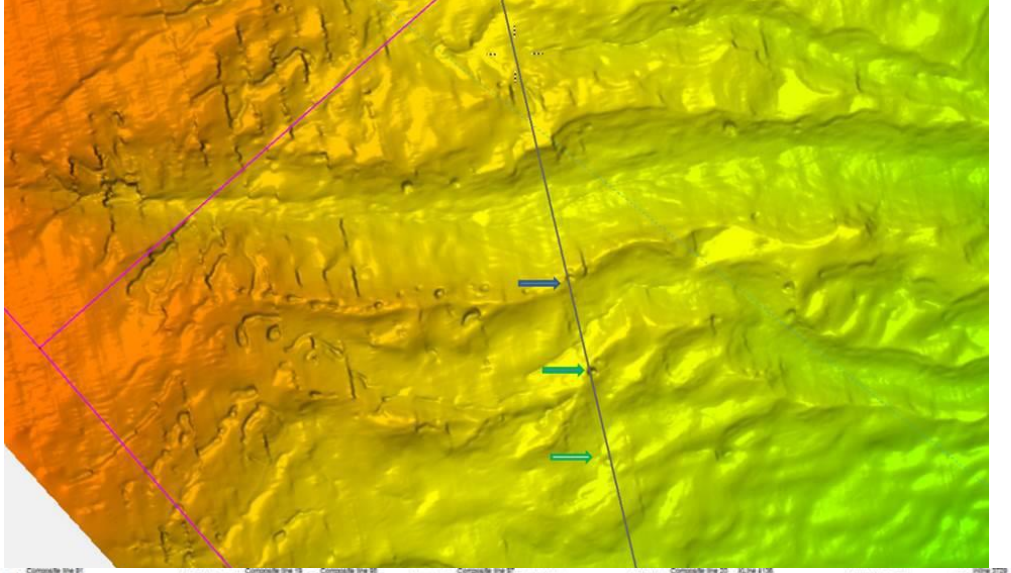

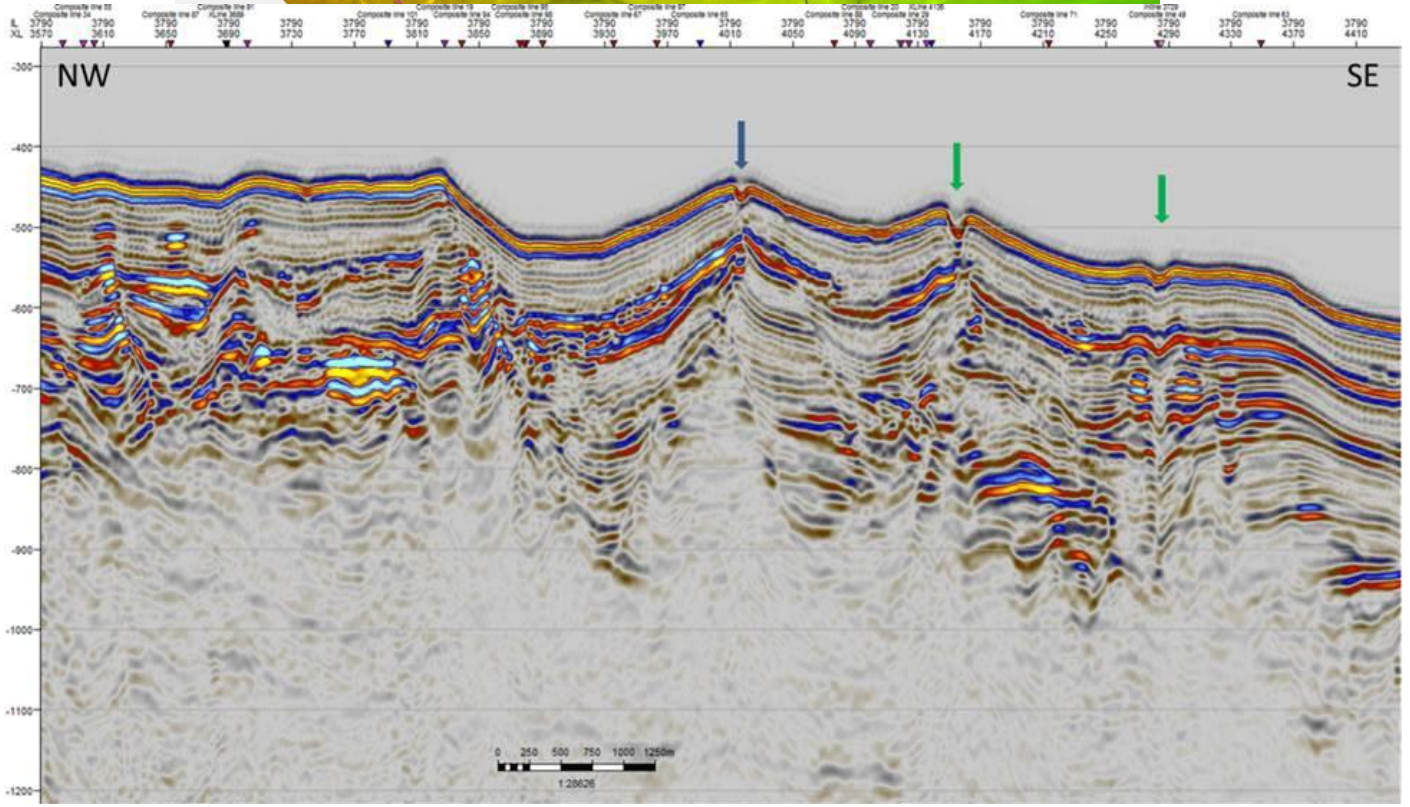

Покмарки (pockmark) на батиметрической карте и на сейсмическом профиле (из сейсмического куба 3Д)